ICE CRUSHING BY IMPACT AND INDENTATION:

A LITERATURE REVIEW

A REPORT

Prepared for

National Research Council of Canada

by

Ian Jordaan and Associates Inc.

St. John's, Newfoundland

Project Team

Ian J. Jordaan

Richard F. McKenna

DSS File No.
XAQ87-00070(021)/A

February, 1988

90-05210/

ABSTRACT

Upon impact and by rapid indentation at moderate confining pressures, the mechanical properties of ice are degraded by the formation of a dense array of microcracks. This damage process and the elimination of the resulting crushed material are addressed in this review. The traditional viscoelastic theories describing the mechanical behaviour of ice in compression are no longer valid when fracture and damage occur; ice is a very brittle material for which the failure is accelerated by the rate of loading, restricted by confining pressure and modified by temperature. There is little evidence that ice is a plastic material; deformation takes place through crushing immediately adjacent to the contact face and by fracture elsewhere. There is no development of a plastic zone in the classical sense. Experience with rocks, ceramics, concrete, metals and glass has shown the importance of fracture and damage processes. Parallels are drawn between these materials and ice for the indentation and impact problems. In this review, emphasis is given to experiments on ice in which brittle behaviour is present. Perhaps the most significant conclusion from these tests is that there is no unique specific energy of ice in crushing; this index is very sensitive to confining pressure and may also depend on other factors such as temperature. Future experimental work on ice should concentrate on the breakdown of the energy expended in the formation of crack surfaces, the dissipation of energy across the crack surfaces and in the motion of the crushed particles. These mechanisms interact to induce dynamic ice loads on ships and structures; peak loads can be better understood from the

damage due to the formation of microcracks. The motion of the crushed ice is presently modelled using a viscous fluid analogy. Further experimentation is recommended to substantiate this theory.

ACKNOWLEDGEMENTS

This contract was administered by R.M.W. Frederking of the Institute for Research in Construction at the National Research Council of Canada on behalf of S.J. Jones of the Institute for Marine Dynamics. The report was reviewed by R.M.W. Frederking and G.W. Timco of the Division of Mechanical Engineering at NRC who suggested many references, particularly relating to experimental studies. M. Sayed of the Institute for Research in Construction provided some constructive comments on the material contained in Chapter 6. Also assisting in the review process were L.W. Gold, L.Y. Shih of IMD and J.S. McCallum of Canadian Coast Guard Northern.

TABLE OF CONTENTS

	Page
Title Page	i
Abstract	ii
Acknowledgements	iv
Table of Contents	v
List of Tables	vii
List of Figures	viii
1. INTRODUCTION AND MOTIVATION	1
2. ICE MECHANICS	3
2.1 Scope	3
2.2 Viscoelastic Theory	4
2.3 Higher Strain Rates and Complex States of Stress	9
3. IMPACT, INDENTATION AND PENETRATION	17
3.1 General Comments	17
3.2 Impact	18
3.3 Classical Indentation and Hardness Tests	27
3.4 Impact and Indentation of Brittle Materials	34
4. ICE INDENTATION AND IMPACT	39
4.1 General Comments	39
4.2 Impact	40
4.3 Indentation Theory	53
4.4 Indentation Experiments on Ice Sheets	56
4.5 Continuous Indentation of Bulk Samples	66
5. DAMAGE PROCESSES IN ICE	68
5.1 Role of Damage Mechanics	68
5.2 The Damage Process	72
5.3 Cracks in Compression	74
5.4 Continuum Damage Mechanics	76
5.5 Non-uniqueness of Stress-Strain Relationships	84
5.6 Energy Effects	87

		Page
6.	FLOW OF CRUSHED MATERIAL	91
	6.1 Evidence of Pulverised Ice	91
	6.2 Geotechnical Properties of Crushed Ice	93
	6.3 Theory of the Flow of Granular Materials	96
	6.4 The State of the Art: Flow of Crushed Ice	100
	6.5 Suggested Procedures for Impact Testing	105
7.	CONCLUDING REMARKS	108
	7.1 Conclusions	108
	7.2 Recommendations	110
8.	REFERENCES	114
	8.1 Textbooks on Impact and Damage	114
	8.2 References Cited in the Report	115
	8.2 Other References on Impact and Damage	124

LIST OF TABLES

		Page
2.1	Hardness tests on single ice crystals.	8
2.2	Experimental results on critical stress intensity factor, K_{IC} of freshwater and sea ice.	10
3.1	Measured Yield Stresses Y and Vickers Indentation Pressures P, in kg mm^{-2}†	29
4.1	Summary of impact tests on ice.	42
4.2	Measured pressures during impact tests	51
4.3	Predicted indentation coefficients for a rectangular indenter using plastic solutions.	55
4.4	Summary of continuous indentation tests on ice sheets.	57
6.1	Summary of shear box tests on broken ice particles.	93
6.2	Summary of confined rubble compression tests by Sayed (1987).	96

LIST OF FIGURES

		Page
2.1	Viscoelastic models for ice.	5
2.2	Creep curves based on the model of equation (2.1).	7
2.3	A typical flaw, propagating under the stress, σ, normal to the crack orientation.	11
2.4	Stress strain curves for uniaxial compression. Slabbing typically occurs in the region of high strain rate outlined	12
2.5	Deviatoric stress, σ_1-σ_3, as a function of confining pressure, σ_3, in triaxial experiments on polycrystalline ice (from Jones, 1982)	14
2.6	Stress-strain curve from Jones (1982) triaxial tests showing accelerating creep.	15
2.7	Uniaxial compression stress-strain curve illustrating creep damage.	15
3.1	Propagation of a stress pulse, showing displacement in the direction of the force represented by f(x) at two instants in time.	19
3.2	Compressive stress wave in a rod.	21
3.3	(a) Stress wave due to a force that is decreasing as in an impact of an object with relatively small kinetic energy and mass; (b) shows refection from a fixed end and augmentation of stress field.	23
3.4	Tensile fracture caused by compressive shock wave.	24
3.5	Elastic-plastic wave propagation.	26
3.6	Creep penetration of ice by a cylinder.	28
3.7	Slipline fields for Hill (1954) plasticity solutions	30
3.8	Increase in volumetric pressure in curved sliplines.	32
3.9	(a) Elastic-plastic indentation in ceramics. (b) Formation of median/radial crack using Vickers indenter and associated residual.	35
4.1	Penetration depth vs impact energy for the impact of projectiles on ice from various sources.	46
4.2	Crushed volume vs impact energy for the impact of projectiles on ice from various sources.	47

Page

4.3 Theoretical indentation coefficients (from Croasdale et al., 1977). 55

4.4 Continuous indentation of a rectangular indenter showing the crushed layer. 59

4.5 Indentation coefficient, p/σ_y, as a function of aspect ratio, D/h. 61

4.6 Oscillating force during continuous indentation showing "sawtooth" pattern (from Sodhi and Morris, 1984) 62

4.7 Map of brittle failure mechanisms for ice in continuous indentation as a function of rate and aspect ratio (from Timco, 1986). 64

4.8 Map of failure mechanisms for ice in continuous indentation as a function of rate and aspect ratio (from Evans et al., 1984). 64

4.9 Microcracking against the face of an indenter during a continuous indentation experiment. 65

4.10 Pressure-area relation from Mobil's spherical indenter tests at Pond Inlet (from Johnson and Benoit, 1987) 66

5.1 Illustration of crushing of ice between solid ice and a structure. 69

5.2 Dynamic force-time relationship and ice crushing. 70

5.3 Cycle loading of concrete in compression based on the work of Spooner and Dougill (1975). 74

5.4 Crack in compression. 75

5.5 Simplified bilnear damage model. 78

5.6 Damage relationships: (a) with memory and (b) without memory of origin. 79

5.7 Energy of pulverisation and subsequent flow of crushed ice. 83

5.8 Strain and stress controlled tests and associated flow of mechanical energy into the specimen. 85

5.9 Non-uniqueness of stress-strain relationship for damaging materials. 86

5.10 Uniaxial stress-strain representation for a purely elastic damaging material. 89

Page

6.1 Typical results from shear box tests. 94

6.2 Schematic showing the behaviour of Bingham "locking", Newtonian and non-Newtonian fluids. 99

6.3 (a) Continuous indentation experiment,
(b) Cross-section perpendicular to the face of the indenter. 101

1. INTRODUCTION AND MOTIVATION

The design of Arctic structures and vessels requires estimates of global and local ice forces. This will involve an analysis of the extreme forces likely to be encountered, and to achieve this, an understanding of how ice fails represents an important step. An appreciation of the mechanics makes it possible to consider appropriate methods to calculate pressure distributions and global loads.

The present report represents an initial stage of a programme of research by the National Research Council of Canada, sponsored by the Canadian Coast Guard. The objective is to investigate the mechanisms involved in the ice crushing part of the interaction of ice with structures or ships. The emphasis is on developing an understanding of the process.

Ice, like any other material, will fail where it is weakest: most engineering experience and analysis is concerned with objects engineered to give the greatest strength. The mechanics of damaging materials is a relatively new area of study in mechanics that has been applied successfully to rocks and concrete. Application of this theory to ice represents a potentially useful approach to peak stresses: the analysis however cannot stop at this point. After pulverisation, the crushed ice will be extruded from the zone between the structure and the solid ice.

Tests of indentation and impact have often been conducted in the context of "engineered materials" noted above. Examples are the indentation hardness tests. Hard indenters such as a diamond pyramid or cone (Vickers and Rockwell tests, respectively), or a hard steel ball (Brinell test) are pressed into flat surfaces of the material, using a standard indenting force. The size of the indentation caused by the indenter is a measure of the hardness of the material. Similarly, impact tests have been used to obtain the properties of materials; an example is the Charpy V-notch test, to test for brittle response.

The tests just noted have a strong empirical basis, and are often used in quality control. The applications have tended to obscure a more detailed understanding of the mechanisms of failure. It is important in ice research to use impact and indentation tests to understand the failure mechanisms and ice clearing processes rather than as an empirical measure of strength. This improved understanding of the phenomena will, it is hoped, point the way to better scaling laws and strategies for ice modelling as well as improved analytical procedures for ice load determination.

2. ICE MECHANICS

2.1 Scope

As noted in Chapter 1, many tests in the area of indentation and impact have been carried out to determine the properties of strong solids such as metals, often using empirical, experience-based techniques. A common property of the materials used in such applications is ductility, based in most cases on a well-defined yield point, and material response that is not sensitive to the rate of load, except at high speed impacts. Ice does not exhibit this kind of behaviour; it is ductile only at low levels of stress, corresponding to low rates of loading, it has no distinct yield point, and it is extremely brittle. It is therefore considered appropriate to review briefly the mechanics of ice. This is intended to assist in putting the subsequent discussion into perspective.

A wide variation in the mechanical behaviour of ice has been observed in laboratory studies; it may depend on temperature, geometry, loading conditions, degree of confinement and ice characteristics. Some important features of this behaviour are outlined in this chapter. The loading conditions at which damage is recipient are also identified; this gives a perspective on what situations cannot be treated using standard creep or viscoelastic formulations.

There are many manifestations of the behaviour of ice that lead to

a picture that is at first confusing; this complexity becomes apparent in reviews such as Michel (1978). Interpretation is sometimes difficult and, in particular, the fact that ice is extremely brittle, points to the need for methods of analysis more specific to ice than conventional continuum theories.

Ice is an elastic, creeping solid, yet it is extremely brittle, one of the most brittle materials on earth. Its brittleness is evidenced by the extremely low fracture toughness and strain energy release rate. The latter value is of the order of 0.5 - 2 J/m^2, similar to the value for glass. The result of this extreme brittleness is a propensity to fracture; stable microcracking is a common occurrence in compressive states, leading to disintegration or pulverisation of ice.

2.2 Viscoelastic Theory

One might consider plasticity theory as a simplification, or special case of creep. If the "flow" takes place at a distinct yield stress, and happens rapidly, then creep can be replaced by "plastic flow". There is no evidence that this is the case for ice, as pointed out by Pounder (1965). The most widely accepted creep law for ice is that proposed by Sinha (1978), given here in terms of the uniaxial creep compliance, for loading at $t = 0$.

$$J(t) = \frac{1}{E} + \frac{1}{E_k}\left(1 - e^{-At^B}\right) + C\sigma^{n-1}t \qquad (2.1)$$

In this, E is the elastic modulus, and E_k, A, B, C and n are constants.

It is attractive to represent (2.1) in terms of a Burgers rheological model (Figure 2.1); this is strictly correct for the elastic and viscous terms, but the delayed elastic term - the second term on the right hand side of (2.1) - cannot strictly be derived on the basis of viscoelastic theory. The power "B" is the reason for this. Other models were reviewed recently by Ashby and Duval (1985) and there appears to be scope for other formulations.

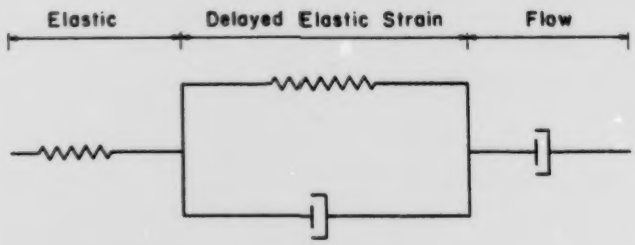

Burgers Body

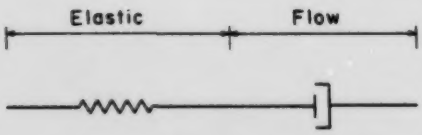

Maxwell Body

Figure 2.1. Viscoelastic models for ice.

It is an interesting fact that a class of models of the kind

$$J(t,\tau) = J_1[\psi(t) - \psi(\tau)], \tag{2.2}$$

where $\psi(\cdot)$ represents a function or "reduced time" that accounts for a range of effects, including non-linearities of stress-strain relationships, can be derived from general constitutive theories (Shapery, 1964). These can be put into a stress-strain relationship of the kind:

$$\epsilon(t) = \int_0^t J_1[\psi(t) - \psi(\tau)] \frac{d\sigma}{d\tau} d\tau \tag{2.3}$$

which is of the form of a Boltzmann superposition model, even though non-linearities are included. Models of this kind, and their use in modelling ice, are reviewed in Jordaan and McKenna (1988, in preparation).

Glen's law, the third term of (2.1), comes into the category just described, with

$$\psi(t) = \int_0^t [1/\mu(\sigma)]\, dt', \tag{2.4}$$

where $\mu(\sigma) = 1/(c\sigma^{n-1})$ is the viscosity of the non-linear dashpot at the instant in time when the stress σ is applied.

It is often appropriate to neglect primary creep (or even elasticity) if secondary creep dominates. The lower part of Figure 2.1 shows the simple Maxwell model which can be used to solve a variety of practical problems.

As noted earlier, there is no clear threshold stress for creep and this is illustrated in Figure 2.2, where curves based on constant strain rate have been calculated. The "yield" plateaux are not unique and depend on the strain rate. These results are confirmed by many experimental data sets.

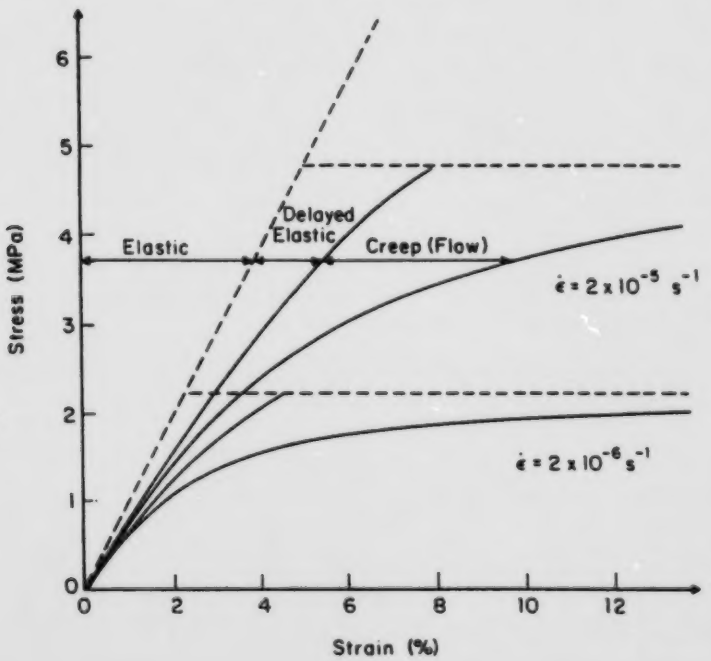

Figure 2.2 Creep curves based on the model of equation (2.1).

Some traditional measures for determining the hardness of metals have been applied to ice. Results for single ice crystals are summarized in Table 2.1. Generally, hardness increased with temperature, although Ackley (1973) noticed a decrease as the temperatures approached 0°C. These tests do not account for the influence of the rate of application of the load and therefore fail to describe a very important aspect of ice behaviour. The basis for these hardness tests is largely empirical; they do little to increase an understanding of ice behaviour.

Table 2.1. Hardness tests on single ice crystals.

Authors	Test Type	Hardness Index	Results
Ackley (1973)	Knoop hardness	KNH=6 kg/mm^2	KNH increases with temperature below -10°C
			KNH decreases with temperature between -10°C and 0°C
Butkovitch (1954)	Brinell hardness	4-17 kg/mm^2	increases with temperature between -50°C and -5°C
	scratch	6-75	increases with temperature between -50°C and -5°C

2.3 Higher Strain Rates and Complex States of Stress

Although ice creeps at any stress state or level, excluding purely hydrostatic states, it is usually dominated by the propensity to fracture. Under tensile states of stress, the critical flaw will propagate at a stress given by

$$\sigma_c = \left(\frac{EG_c}{\pi a}\right)^{1/2} \tag{2.5}$$

where E = elastic modulus, G_c = energy requirement per unit area of crack, and is essentially a material constant (for a given stress state) and a = half the crack length. A typical crack is shown in Figure 2.3. The critical flaw will have the combination of length and orientation which gives the lowest value of σ_c for all cracks in the sample of material in the body under consideration. At lower stresses, the material will creep without fracture. Generally, the critical crack will propagate right through the specimen, leading to failure. The value of G_c is determined by experiment and depends on the stress state, which affects the ease with which a crack will propagate.

Experiments in which the critical stress intensity, K_{IC}, has been evaluated are summarized in Table 2.2. This is a measure of fracture toughness that includes the elastic modulus and is given by

$$K_{IC} = (EG_c)^{1/2}. \tag{2.6}$$

Table 2.2 Experimental results on critical stress intensity factor, K_{IC} of freshwater and sea ice.

Authors	Ice Condition	Test Type	Rate of Test $\dot{K}_{IC}$ (kPa $m^{1/2} s^{-1}$)	K_{IC} (kPa $m^{1/2}$)	Results
Timco and Frederking (1986)	Fresh Columnar -10°C	3 pt and 4 pt bending	6-80	90-150	decreases with increase in stress rate, grain size and crack density
Hamza and Muggeridge (1979)	Fresh, Columnar, -40°C to -4°C, 8 mm-12 mm grains	3 pt bending	0.1-50	40-160	decreases with increase in stress rate and temperature
Urabe et al. (1980)	Sea ice -2°C	3 pt bending	1-2000	40-100	increases with increase in grain diameter decreases with increasing stress rate
Goodman (1980)	fresh, poly -24°C, -11°C, -4°C	4 pt bending	200-4000	45-185	no temperature dependence
Parsons and Snellen (1985)	fresh -20° to -15°C	double cantilever	2-100	100-500	no decrease with rate
Liu and Miller (1979)	fresh -46°C to	30° wedge	0.1-2000	80-400	increases with loading rate decreases with temperature

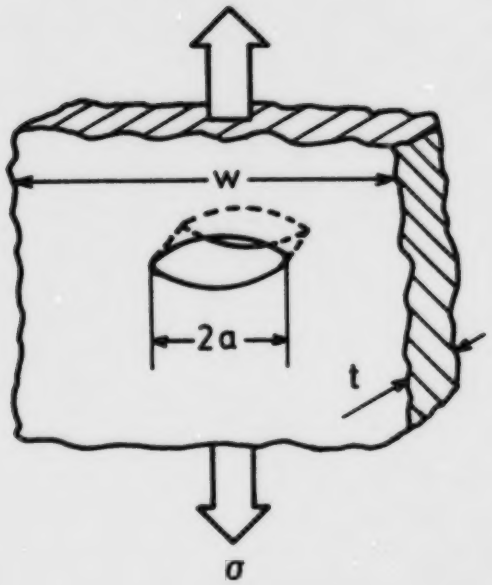

Figure 2.3. A typical flaw, propagating under the stress, σ, normal to the crack orientation.

The reported range of K_{IC} values of 50 to 200 MPa $m^{1/2}$ translates into a fracture toughness, G_c, of 0.5-2 MJ m^{-2} for an elastic modulus, E, of 10 GPa.

Under compression, cracks are somewhat less prone to propagate completely through the specimen. Some microcracking generally occurs before failure. The phenomenon of "slabbing" is observed at higher strain rates; this is seen in most brittle materials such as concrete, sulphur, glass and ice. A single crack propagates right through the specimen, parallel to the direction of loading. This is also seen in quite large scale tests (Wang and Poplin, 1981).

Figure 2.4 illustrates schematically the stress-strain response of ice in compression, as it relates to a variety of phenomena. The figure is based on results in the literature and the key features as regards the material response are also illustrated. As the strain rate increases, pure creep becomes less important, microcracking is observed and the curves and the tests are often terminated by cracks that extend vertically from the top to bottom of the specimen, the "slabbing" phenomenon as noted above (Ashby and Hallam, 1986).

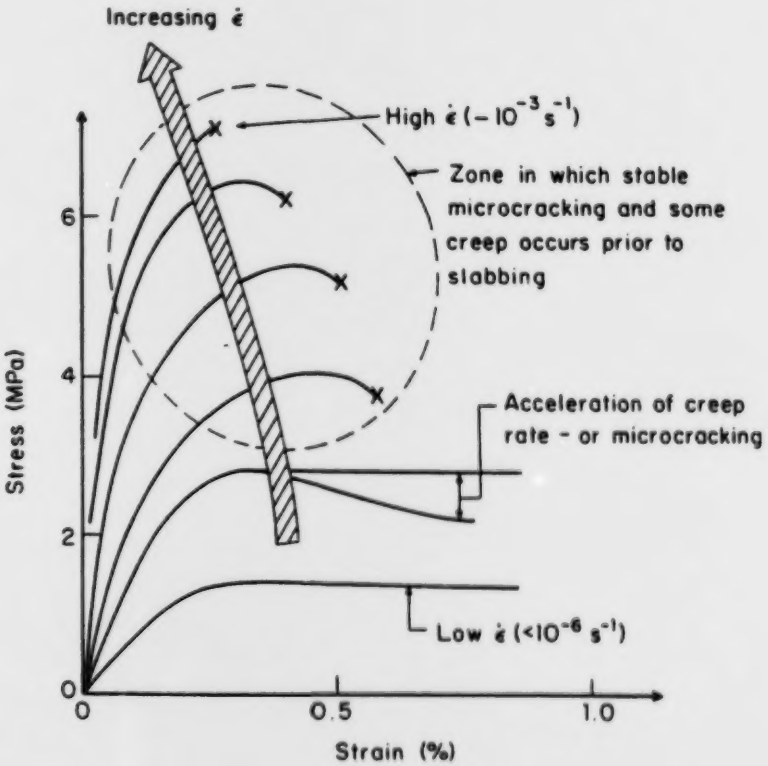

Figure 2.4 Stress strain curves for uniaxial compression. Slabbing typically occurs in the region of high strain rate outlined.

In practice, ice is frequently confined by its geometry and does not fail as above. This has been tested on small samples using a triaxial setup with a normal pressure, σ_1, and a confining pressure, σ_3. If creep is independent of hydrostatic pressure (equivalent to the confining pressure in this case), then the excess of normal pressure over the confining pressure, σ_1-σ_3, should be independent of σ_3. The maximum deviatoric stresses, σ_1-σ_3, obtained by Jones (1982) in triaxial tests of polycrystalline ice are plotted as a function of confining pressure, σ_3, for different strain rates in Figure 2.5. Most of the dependence of deviatoric stress on confining pressure is found in the shaded region in which confining pressures were low and strain rates were high. These are conditions under which damage can occur. The numbers may vary for different ice types but the concept that confining pressure can inhibit damage to the sample in the propagation of microcracks is important.

A couple of examples from experiments are described to show that the stress-strain curve for ice in compression is far from being unique. Jones (1982) observed the process of accelerating creep in Figure 2.6 under a triaxial stress state. A significant fall in the stress-strain curve occurred without any apparent damage to the sample. This was attributed to an increased number of dislocation sites. Consider in contrast, the recent results of a test concluded at

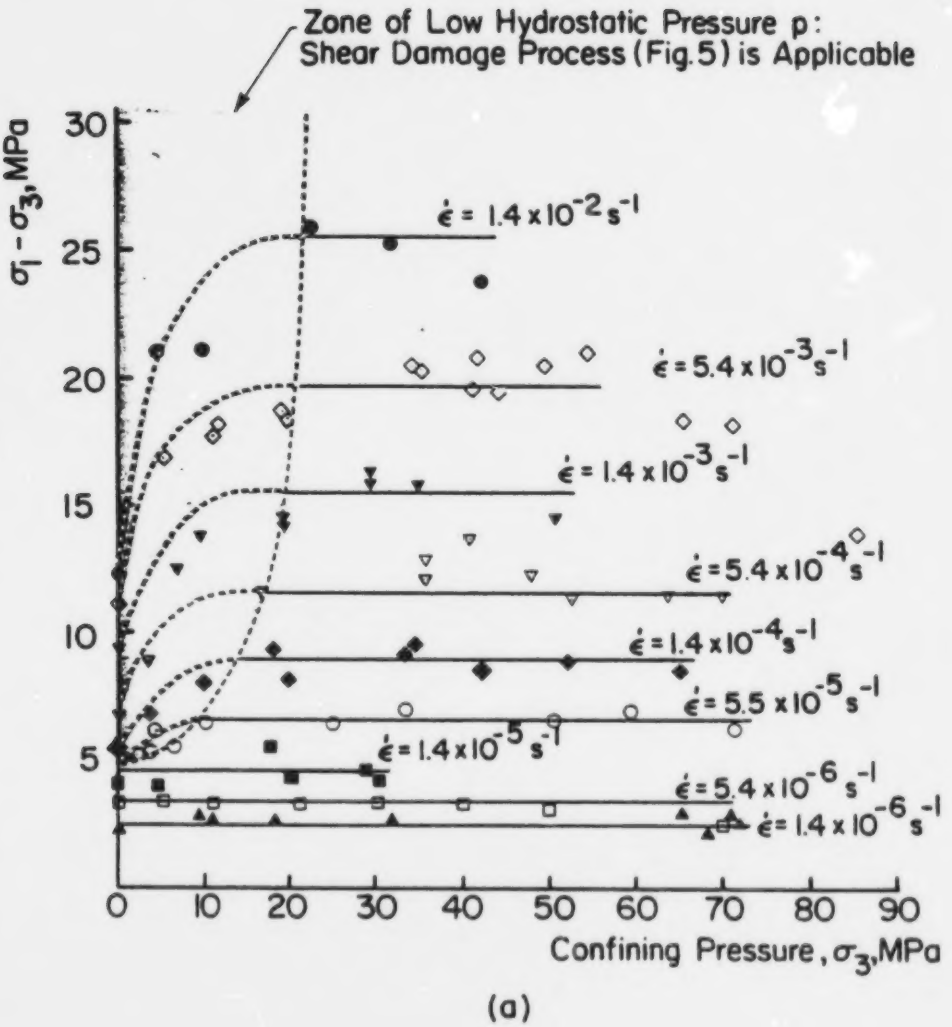

Figure 2.5. Deviatoric stress, $\sigma_1 - \sigma_3$, as a function of confining pressure, σ_3, in triaxial experiments on polycrystalline ice (from Jones, 1982).

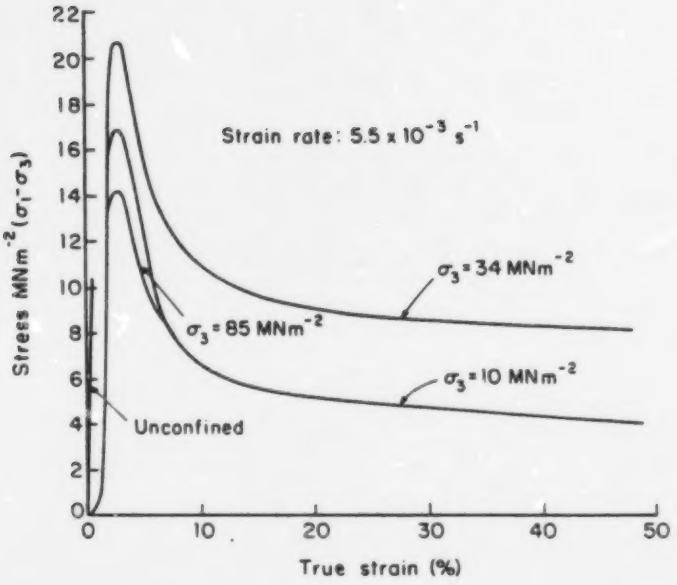

Figure 2.6. Stress-strain curve from Jones (1982) triaxial tests showing accelerating creep.

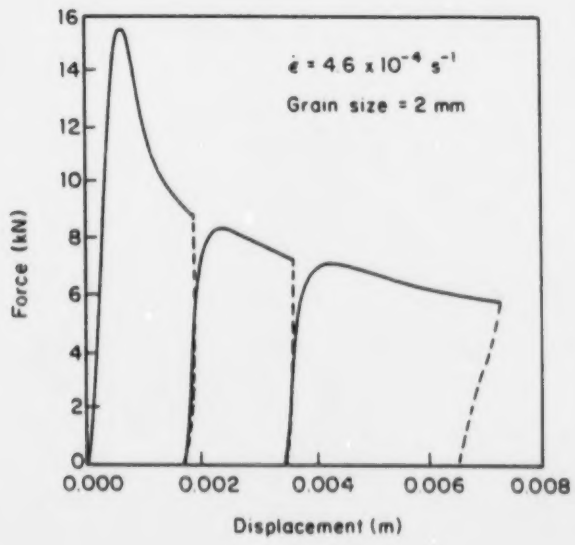

Figure 2.7. Uniaxial compression stress-strain curve illustrating creep damage, then stabilization.

Memorial University of Newfoundland for uniaxial compression in Figure 2.7; the same shape of curve was observed, yet there was considerable damage to the specimen. Unloading and reloading of the specimen showed little change in the elastic properties as creep damage progressed.

To conclude this chapter, creep analysis is appropriate for low strain rates and also at higher strain rates with confining pressures sufficient to suppress the propagation of microcracks. The occurrence of microcracking under moderate compression is an area of great practical concern since this is the principal mechanism involved in the "ice crushing" process. Damage has been found to increase with strain rate in uniaxial and confined compression tests and to decrease with confining pressure. This latter effect is appropriate for confining pressures of up to 30 MPa. The influence of temperature on crack formation and damage accumulation has not been well defined as the ice approaches its melting point, particularly at fast loading rates. Theories for damaging materials and their application to ice are further addressed in Chapter 5.

3. IMPACT, INDENTATION AND PENETRATION

3.1 General Comments

Impact generally is concerned with the sudden application of load, for instance in the collision of two bodies. As far as testing is concerned, this is often achieved by the following:

- dropping objects onto the surface of the object or material to be tested
- attaching a mass to a pendulum and permitting it to rotate freely until impacting the object or material to be tested.
- firing projectiles at the surface of the material to be tested.

The distinguishing feature of impact tests is that the impacting objects have a distinct kinetic energy upon contact with the surface of the material or object being tested.

Indentation tests, on the other hand, involve pressing or pushing an object into the surface of the test material. This can be achieved by pressing until a specified force or displacement is attained. In these instances, the test terminates once the specified condition is achieved. A further kind of indentation test is the continuous indentation test, in which the indenter moves continuously through the test specimen. This is commonly used in ice testing, with indenters of

various shapes (rectangular, circular in cross section) pushed through an ice sheet. In continuous indentation, either the speed is kept constant, with the load being measured as a function of time or alternatively a constant load can be applied with measurement of displacement as a function of time.

The two alternative controls of load or displacement are common also in compression testing of samples in which results with stress or strain control are commonly reported. The possibility of combining load and displacement and to control energy is an avenue that should be explored. In impact tests, the incoming energy is controlled. This energy is either dissipated in the impact or may be converted again to potential or kinetic energy, for instance in the energy associated with rebound.

In most impact and indentation tests, the indenter is regarded as being rigid. Elastic movements, including flexing of the support devices in indentation tests, can have a significant influence on the ice response. In the latter case, elastic strain energy is alternately stored in the device, then flows into the ice. This will clearly affect the ice response.

3.2 Impact

Problems of impact are necessarily concerned with the propagation of stresses and strains in the material of concern. For simplicity, we

consider a rod of material, stressed initially at one end. Any stress pulse (sound wave or water packet) will propagate along the rod, with the size and shape depending on the initial disturbance. Figure 3.1 illustrates the fact that the wave moves without change of shape or size. The velocity of the wave c_L is given by

$$c_L = \left(\frac{E}{\rho}\right)^{1/2} \tag{3.1}$$

where E = Young's modulus and

ρ = density of the material.

For ice, this equation yields values of the order of 3300 m/s.

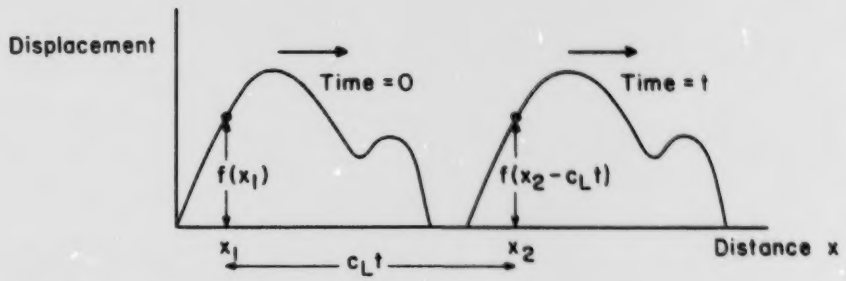

Figure 3.1 Propagation of a stress pulse, showing displacement in the direction of the force represented by f(x) at two instants in time.

More generally, we can consider any two conjugate components T and ϵ e.g. a shear stress and shear strain which correspond to the mode of deformation being considered, with a relation of the following kind:

$$T = f(\epsilon).$$

The longitudinal wave speed is given by

$$c_L = (\frac{1}{\rho} \frac{df}{d\epsilon})^{1/2}.$$

In the interior of an elastic solid, longitudinal expansions and contractions occur, but with the transverse motions restricted, resulting in the formula

$$c_L = [\frac{E(1-\nu)}{(1+\nu)(1-2\nu)\rho}]^{1/2} \qquad (3.2)$$

where ν = Poisson's ratio.

In the case just discussed, the speed calculated for the rod is enhanced by about 20% resulting in a value of about 4000 m/s. This is based on a value of ν=0.33. Transverse and Raleigh surface waves will not be considered here, but the speeds are generally of the same order of magnitude as the others.

The speeds just calculated are orders of magnitude greater than

the speeds of impacts envisaged in arctic navigation, or indeed in ice-structure interaction. Nevertheless, they are useful in delineating a zone of elastic stress for the calculation of the deformation of the contact area due to elastic stressing of an ice mass. This contact area will deform and rebound during variations in load and could contribute to the ejection of crushed ice (section 6.4). The stressed zone is illustrated for a rod in Figure 3.2; for a more general shape of object being deformed, the state of stress must be accounted for in delineating the zone.

The transmission of a stress wave in a material can lead to some interesting effects. Let us consider initially a prismatic bar, Figure 3.2, one end of which is suddenly put into motion with a constant velocity v. The stress wave has a front, denoted B in Figure 3.2, such that all material to the left is stressed and in motion with the

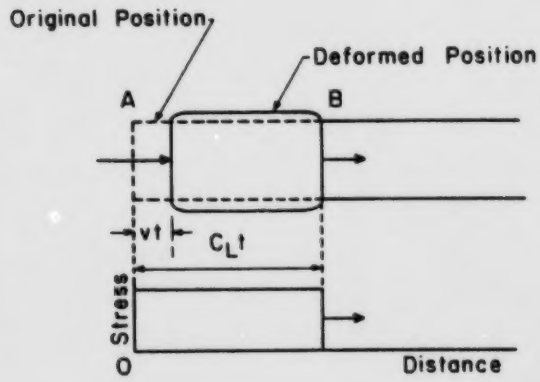

Figure 3.2. Compressive stress wave in a rod.

material to the right unstressed and at rest. At time t, a length ($c_L t$), of mass ($\rho A c_L t$), where A is the cross section area, is in motion at velocity v. The momentum is ($\rho A c_L tv$) and the force associated with this momentum is its time derivative, ($\rho A c_L v$), giving a stress

$$\sigma = \rho c_L v. \tag{3.3}$$

Eliminating ρ from equations (3.1) and (3.3), it is found that

$$\sigma = \frac{Ev}{c_L} . \tag{3.4}$$

From equation (3.4) it is seen that the stress depends initially on the velocity of impact. If the impacting object has a mass m, then the impacting force will cause the object to slow down, thus decreasing v. For a large object, this takes some time: during the initial period, the stress depends on v and not on m. In the case of ice, we may take the compressive strength of a small sample as (E/1000); the speed corresponding to this limiting stress is then seen from equation (3.4) to be $c_L/1000$ or about 3-4 m/s. The implication of this is that speeds of impact greater than 3-4 m/s would generate failure in the ice that is speed-dependent and independent of mass, an interesting prospect for icebreaking.

If the finite speed of stress propagation is ignored, the usual analysis of dynamic stresses on the basis of energy exchange can be carried out, assuming the stresses and consequently strain energy to be

developed instantaneously.

Let us consider now the reflection of stress waves. A specimen that is clamped at its far end will reflect a wave. Figure 3.3 shows an object dropped onto such a clamped specimen. After the initial impact the stress wave will diminish in intensity as the object decelerates: reflection from the other end can cause the stress to rise considerably, possibly resulting in failure. A classical paper in this area is by Taylor (1946). The reflections can repeat from one end to the other and build up, given similar (fixed) boundary conditions.

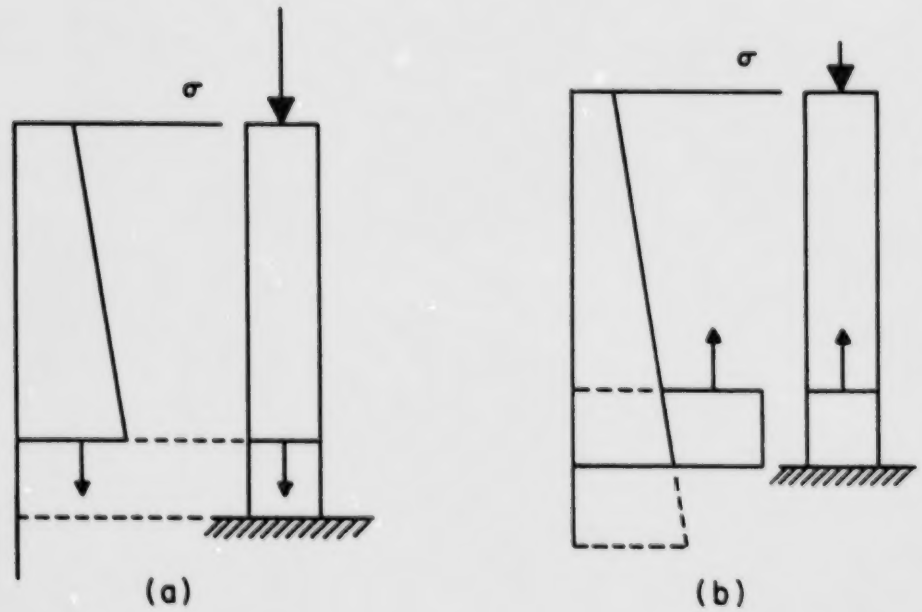

Figure 3.3. (a) Stress wave due to a force that is decreasing as in an impact of an object with relatively small kinetic energy and mass; (b) shows refection from a fixed end and augmentation of stress field.

For a free condition at the far end, appropriate for the edge of an ice floe, the reflected wave has an opposite sign to the incident wave and cancels it out.

An interesting effect occurs when a compressive pulse of finite duration is imposed on a body with a free edge at the "far" end. A tensile pulse is reflected, which cancels the incident compressive pulse while the two pulses overlap at the end of the object, near the free (far) end; after this, a tensile stress occurs near the free end. If this exceeds the tensile strength of the material, failure will take place, illustrated in Figure 3.4. Has this been observed in ice? Johnson (1972) discusses various cases where this effect has been

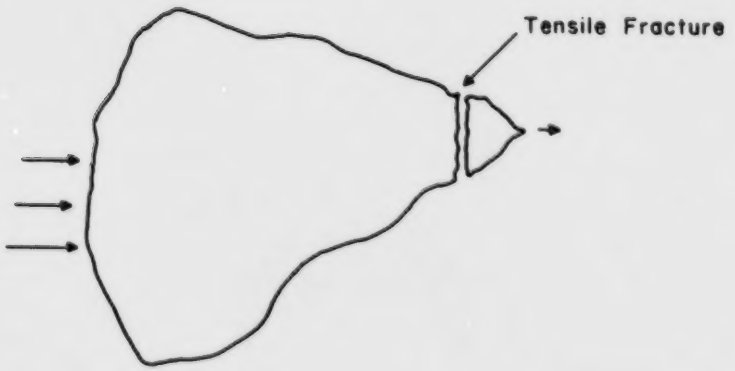

Figure 3.4. Tensile fracture caused by compressive shock wave.

observed: in concrete and rocks (both weak in tension) such failures have been induced, in situations involving impact, particularly with the use of explosives. Sudden changes in load can result from the fracture processes themselves and there may be shock waves that result.

In the above, consideration has been given to elastic waves, and to the effect of tensile stresses that exceed the material strength. Apart from this, material behaviour has not been discussed. Plastic material response has been studied in some depth, with major wartime contributions becoming public in the late 1940's. The general principle is illustrated in Figure 3.5. Consider a material with a yield stress σ_y and a bilinear stress-strain curve as shown in Figure 3.5(a). If the stress applied to the bar shown in Figure 3.5(b) exceeds σ_y two waves are propagated, first an elastic wave at a speed $c_L=\sqrt{E/\rho}$ and second, a slower "plastic" wave at $c_p=\sqrt{F/\rho}$ where F is the modulus in the strain hardening region.

It is maintained in the sequel that, in compression, ice is a damaging material (at least at the higher strain rates of concern) and does not exhibit plastic behaviour. The postulated behaviour is the progressive destruction of the stiffness, particularly shear stiffness. This would result in a decrease in the ability of the material to transmit shear waves. The decreasing modulus would result in slower speeds. Increasing shear degradation would result in the absence of shear wave transmission; only pressure effects associated with volumetric stresses would remain.

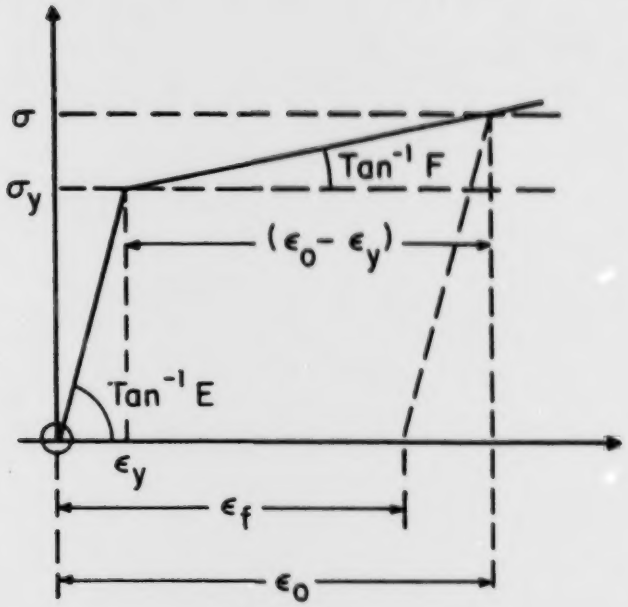

(a)

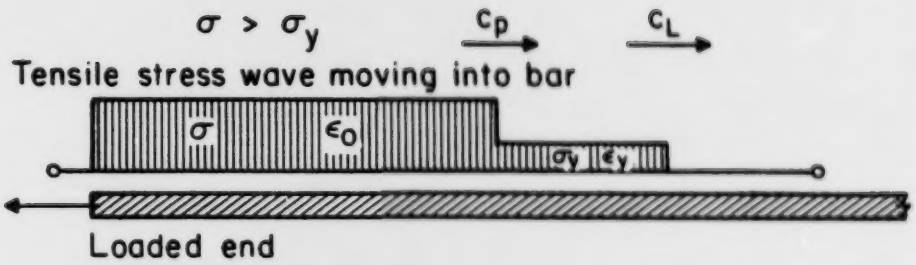

(b)

Figure 3.5 Elastic-plastic wave propagation
(a) stress-strain relationship,
(b) wave moving through bar with two fronts

3.3 Classical Indentation and Hardness Tests

It has been noted in Chapter 1 that indentation tests, such as the Vickers, Rockwell and Brinell tests, are used to determine the hardness of materials by pressing a hard indenter into the surface of the material with a specified (standard) force. The size of the indentation gives a measure of hardness. The empirical use of hardness tests has been used for various practical objectives; for instance J.A. Brinell proposed the following:

Tensile strength = Constant × Brinell hardness.

Boklen (1973) proposed tests to obtain ductility or percentage elongation from a cone impression; the variety of tests based on indentation is considerable.

For small loads, the deformation is elastic and disappears on removal of the load. This was the problem first studied by Hertz, who analyzed the elastic contact between two curved bodies. The elastic stress field solutions that are available (Hertz, Boussinesq, Michell, for example) have been summarised by Lawn and Wilshaw (1975) and are also discussed in some detail with regard to applications in ice mechanics by Tomin et al. (1985). The latter work also includes a finite element analysis of ice sheets: an elastic analysis can readily be generated by numerical means for awkward geometries, and indeed for contact problems with large deformations if required.

When the load is increased beyond the elastic limit, creep or plastic flow will take place in ductile materials. Figure 3.6 shows a typical creep deformation of a material (such as ice) with a power law creep curve (the contours were generated by a finite element analysis). The depression caused by the load is permanent. This is also the case for plastic flow, in which case the irreversible deformation occurs at a certain yield stress, or occurs above this value for strain hardening materials.

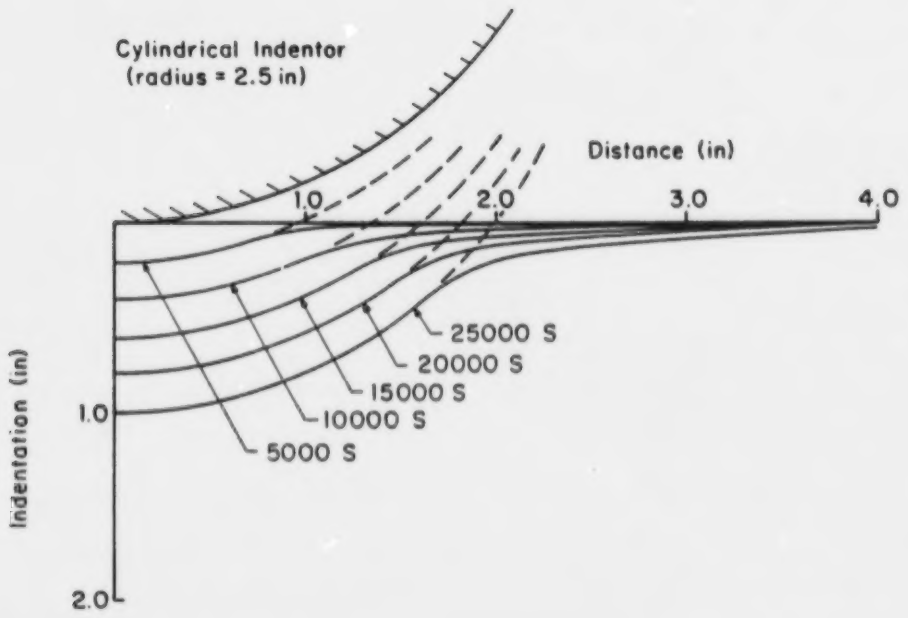

Figure 3.6. Creep penetration of ice by a cylinder.

Since plasticity solutions have had a strong influence on the analysis of ice (incorrectly in the authors' view) this theory will be reviewed briefly to put subsequent work in perspective. Considering first hardness tests, an analysis of experiments shows that the ratio of mean pressure to uniaxial yield stress is about 3; see for example Table 3.1. This follows also from plasticity theory (Hill, 1950, Chapter IX). Two slipline fields are shown in Figure 3.7. The solution for the two cases is similar, the Prandtl field being more appropriate when the indenter surface is sufficiently rough.

TABLE 3.1

Measured Yield Stresses Y and Vickers Indentation Pressures P, in kg mm^{-2}†

Material	Y	P	P/Y
Lead	2.1	6.7	3.2
Aluminum	12.3	39.5	3.2
Copper	27	88	3.3
Steel	70	227	3.2

†D. Tabor, The Hardness of Metals, Oxford University Press, London, 1951.

The collapse load, on the basis of plane strain and rigid-plastic conditions, is relatively easy to obtain. For plane strain, the strain and strain rate out of the plane of Figure 3.7 is zero, therefore

$$\sigma_3 = \tfrac{1}{2}(\sigma_1+\sigma_2), \tag{3.5}$$

where σ_1 and σ_2 are the principal stresses in the plane of the figure (σ_1 being numerically the greater), and σ_3 is the principal stress out of the plane of the figure. Equation (3.5) results from the fact that the strain rate in the third direction is zero; thus σ_3 must generate strain rates equivalent to half of σ_1 and σ_2, since Poisson's ratio is 1/2 for plastic flow.

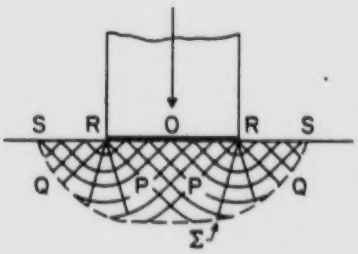

(a)

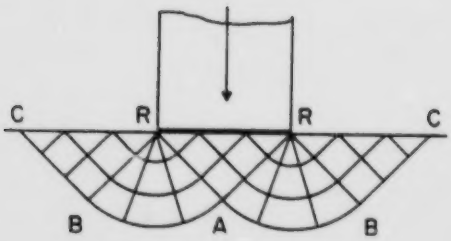

(b)

Figure 3.7. Indentation of a semi-infinite medium by a flat die: plastic region and sliplines (a) Hill's solution, (b) Prandtl's solution.

Under the indenter, which we will consider to be smooth and frictionless, the principal stresses are vertical and horizontal, with a value, q, say, in the vertical direction. In the free surface, the same applies, except that the vertical stress is zero. The state of stress in a plastified (rigid plastic) material in a condition of plane strain is

$$\begin{aligned} \sigma_1 &= -p+k \\ \sigma_2 &= -p-k \\ \sigma_3 &= -p \end{aligned} \qquad (3.6)$$

where p = hydrostatic pressure and

k = shear stress at yield.

Note that, for $\sigma_1 = 0$ on the free surface, the hydrostatic pressure is equal to the shear stress at yield.

The change in pressure around a curved slipline is

$dp = 2kd\phi$,

found by taking moments about 0 (Figure 3.8).

The sliplines in Figure 3.7 rotate through $\pi/2$ so that the hydrostatic pressure under the indenter must be increased by $2k(\pi/2)=k\pi$ above the value at the surface, deduced above to be p=k. Hence the hydrostatic pressure under the indenter is $p=k+k\pi=k(1+\pi)$. The normal stress q (taken as positive in compression) is the second of the set of

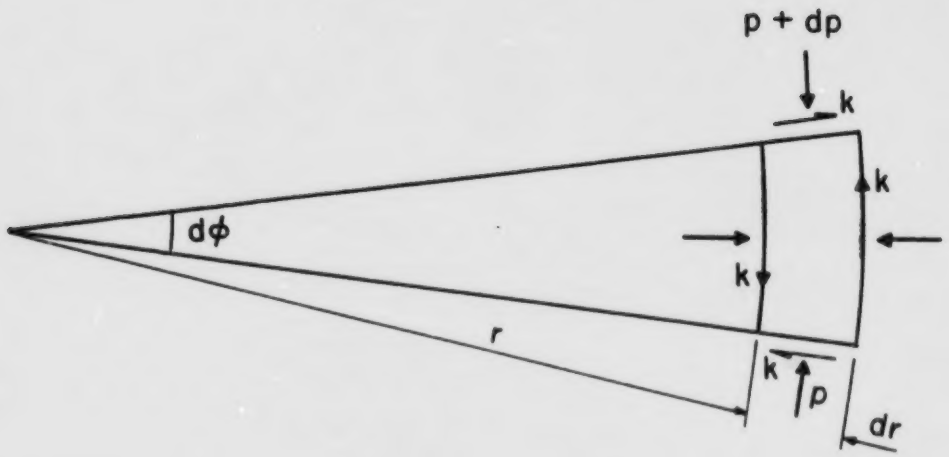

Figure 3.8. Increase in volumetric pressure in curved sliplines.

equations (3.6), since σ_1 is the numerically greatest (tension being positive); i.e. q is given by

$$q = -\sigma_2 = -(-p-k) = (2+\pi)k.$$

For a von Mises material, the yield stress in uniaxial tension σ_y is equal to $\sqrt{3}k$, so that the normal stress under the indenter is

$$q = \frac{(2+\pi)}{\sqrt{3}} \sigma_y = 2.97\ \sigma_y \qquad (3.8)$$

which agrees very well with the measurements noted above. For a

plastic material the normal stress in pushing an indenter into a plane surface is three times the uniaxial strength.

It is important to notice that in the plastic analysis, energy is dissipated a considerable distance from the indenter; the slip lines are in fact planes along which energy is dissipated in shear movements (of dislocations). The material atomic bonds are restored after the movement and the material remains intact; this is a vital distinction with regard to damaging materials. We have dwelt on this theory because it has been widely used to model ice behaviour and in particular to deduce the "equivalent strain rate", $\dot{\epsilon}_m$, variously given as

$$\dot{\epsilon}_m = \frac{V}{4D}, \frac{V}{2D} \text{ or } \frac{V}{D} \tag{3.9}$$

in the literature; V = velocity of indenter and D = diameter or width (a characteristic dimension).

The origin of the expressions is not entirely clear but some guidance can be obtained from Hill's analysis of indentation (Hill, 1950, pp.260-261). First note that for indentation at a constant strain, rather than strain rate, we can consider strain ϵ, and rather than velocity V, we can consider penetration of the surface, δ. Hill wrote the "mean equivalent strain" (for annealed or lightly pre-strained metals) in the form

$$q = \text{constant } \sigma_y(\epsilon_m) \tag{3.10}$$

where the $\sigma_y(\epsilon)$ is the stress-strain relationship based on uniaxial conditions; the constant is again about 3. The equivalent strain can be related to the penetration, or equivalently to the impression diameter d in the case of indentation with a sphere (e.g. the Brinell test). Indeed, in the case of the Brinell test, Hill shows that in the case of annealed copper

$$\epsilon_\mu \simeq .15\ (d/D)\ ;$$

for a die of constant width, (δ/D) replaces (d/D) and the basis for the form of equations (3.9) becomes clear. The deformation of the indenter is "averaged" over a distance αD where α = 1 to 4, in all cases over a considerable distance from the indenter. This is not at all appropriate for the actual localised damage processes in ice at higher indentation rates. It may be used for indentation at very slow rates (Ponter et al., 1983) via the approximate reference stress method; this is relevant to structures in slowly moving ice fields, for instance structures in the landfast ice region of the Beaufort Sea.

3.4 Impact and Indentation of Brittle Materials

Before turning to ice, indentation and impact of other brittle materials will be briefly reviewed. An excellent overall review of indentation fracture is given by Lawn and Wilshaw (1975). States of stress in elastic materials are well discussed; in generalising, a

plastic zone under the indenter was identified (Figure 3.9(a)) and this has been used extensively in the analysis of indentation of ceramics, and will be discussed in more detail below.

When turning to fracture, the analysis by Lawn and Wilshaw concentrates for the most part on tensile cracks forming outside, or propagating from the zone of inelastic deformation (Figure 3.9(b)). These are tensile cracks analysed on the basis of Griffith theory. The question of damage is only dealt with in the context of wear, abrasion and the conscious production of particulate material by fragmentation

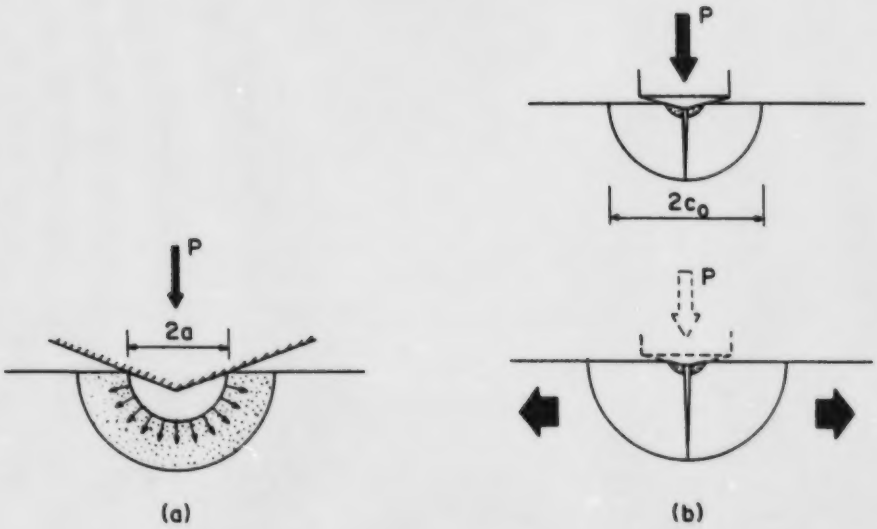

Figure 3.9. (a) Elastic-plastic indentation in ceramics. Dark region is "hydrostatic core".
(b) Formation of median/radial crack using Vickers indenter and associated residual.

(comminution). The formation of ring cracks in silicate glass was studied by Tillett (1955) who conducted a series of experiments on the theme of tensile cracks, initial flaws and size effects. Since crushing and damage were not considered this will not be discussed in further detail.

In reviewing the literature in damage mechanics applied to rocks, concretes and ceramics, a pattern similar to that found in the study of ice is apparent: the permanent impressions observed in the impact region are similar to those found in indentation tests. The continuing mesmerisation of members of the solid mechanics community with plasticity theory has had an influence: for instance Forrestal, Longcope and Norwood (1981) and Forrestal and Longcope (1982) use models based on plasticity theory to analyse the impact of high speed penetrators into concrete, dry rocks and sea ice. Indeed, the last mentioned paper even attributes such plastic properties to sea ice, and predictions and theory were compared for penetrators that were air-dropped into sea ice. No doubt, the result could match the measured decelerations by the use of appropriate constants, but the simulation of a process that involves destruction of material integrity with a theory that does not recognise this disintegration (in fact, recognises only dissipation without damage) hardly improves our understanding of the physics of the process.

A series of papers on indentation and damage (including plastic damage!) in ceramics (Lawn and Wilshaw, 1975; Marshall and Lawn, 1980;

Lawn, Evans and Marshall, 1980; Cook and Lawn, 1984; amongst others) have focussed on a testing technique that consists of the creation of a radial crack by means of a Vickers indenter (Figure 3.9(b)). The presence of a residual stress field was postulated, as a result of plastic flow in the region below the indenter. This material imposes a residual stress if it flows plastically (with no volume change) and is then under a state of compression upon unloading, a "mis-match" caused by the plastic flow on loading. The zone in compression then imparts a tensile force on the surrounding ice, and in the analysis, this effect is included in the stress intensity factor for the crack under the plastic zone. The analysis just described can be used for studies of subcritical crack growth, i.e. extension of the crack below the critical Griffith stress, and for the determination of the speed of crack propagation.

Naturally, creep in ice would tend to diminish the residual stress effect; a more serious criticism is the neglect of damage to the brittle material in the "plastic" zone. A zone of damaged ice would impose no residual stress. In this regard Liaw et al. (1984) presented an excellent analysis of the situation and suggest that for ceramics, a damage model is indeed necessary. They demonstrated the use of a finite element continuum damage model. This provided excellent agreement with experimental results. Above all, an approach to material disintegration based on the actual damage process was taken.

In studies of the disintegration of rock under impact loading, a

team of researchers at Stanford formulated a truly impressive model of progressive damage (Shockey et al. 1974, and Barbee et al. 1972 represent typical works).

They considered very high rates, including tensile shocks with rise times of the order of tens of nanoseconds, and durations of the order of several tenths of a microsecond. These need not be the concern of the present report, since much slower impacts are being considered. Nevertheless, the principles and the approach are, in the authors' opinion, of great value.

Observations on impacted specimens using fractographic methods revealed four stages:

(1) activation of inherent flaws;

(2) growth of cracks;

(3) coalescence of cracks; and

(4) fragmentation.

If one adds the flow and ejection of pulverised material, one is close to the entire problem of ice crushing and clearing! The work of the Stanford group offers a real ray of light; one would want, perhaps, to carry out somewhat less theoretically oriented research in the case of ice so as to fulfill practical objectives. Yet the overall structure is an excellent guide.

4. ICE INDENTATION AND IMPACT

4.1 General Comments

Although mathematical theories have been proposed to consider ice behaviour during indentation, there is a tendency to ignore the basic processes for the sake of mathematical orthodoxy. Ice is a unique and very brittle material; emphasis is therefore placed on the results of laboratory and field experiments.

Because of the large number of test results published, it was necessary to limit the scope of the review. First of all, a minimum impact or indentation speed to produce brittle damage in the form of crushing or fracture was a requirement. This was not always an easy distinction, since the transition between creep and brittle mechanisms is not abrupt. Basically, if creep was the dominant mechanism, the tests were ignored. The emphasis of this review is on experiments in fresh and salt water. Experiments on special model ice were included when the results were of a fundamental nature.

The testing methods reviewed were diverse, but two basic types were noted. Impact is the result of a projectile of known initial energy striking an ice sample. The energy dissipated is evaluated by quantitative assessments of the final state of the ice or by measurement of the energy transmitted through the sample. Examples of these projectiles are steel balls, impact hammers, gun or cannon fired

projectiles and air-dropped projectiles. In contrast, energy is continuously applied during indentation in which the force of an indenter typically applied at a constant velocity is measured.

If there were a single parameter that adequately described ice indentation and impact, then it would certainly have been discovered by now. Crushing strength, while attractive as an engineering design parameter, depends on temperature, loading rate, geometry and degree of confinement. For this to be a valid index, peak pressure must be referenced to a specific mechanism. Few experiments have been described with this in mind.

A frequently used index for describing the response of ice to impact is the energy required to damage a given volume of ice, termed the specific crushing energy. Unfortunately, this also depends on the above factors. As yet, no conclusive experimental evidence exists to relate the maximum impact pressures to the specific mechanisms of elastic deformation, fracture, frictional processes and clearing of pulverized ice particles.

4.2 Impact

Impact tests are defined here as those in which a projectile contacts the ice with a given velocity, but no further force is applied (except perhaps gravity) for the duration of the contact. It is difficult to define the concept of a strain rate in this type of test

since the actual damaged layer changes in thickness during the course of the test. The global picture is defined by the energy or momentum of the projectile prior to impact (e.g. Holsapple and Schmidt, 1982). If the size of the projectile is of any consequence, then the initial energy per unit projected area might be more representative.

The results of laboratory and field dropped weight tests, air-dropped projectile perforation through ice covers and high speed projectile impacts are summarised in Table 4.1 and described in this section. These results are generally reported in terms of the dimensions of the damaged or modified area, the deceleration of the projectile, the recoil force and the pressure distribution on the face of the indenter. If impact were dominated by a single mechanism such as fracture, then the dimensions of the damaged area would yield a useful specific energy of fracture. Recently, Jordaan and Timco (1987) have estimated that frictional forces in the expulsion of pulverized material from the an indenter surface consume much more energy than does the initial microcrack formation. The geometry of the cratered or damaged zone is not therefore conclusive in describing the impact.

Specific energy is a measure of energy density that is defined for impact testing as the ratio of the input kinetic energy and the volume or mass of the damaged material. It is a convenient index of the

Table 4.1. Summary of impact tests on ice.

Authors	Ice Conditions	Impact Type	Impact Energy (J)	Specific Energy (MJ/m^3)
Itagaki and Sabourin (1980)	freshwater -32^{o} to $-2^{o}C$	standard charpy	.035-.05	.006-.01
Kheisin and Likhamanov (1973) Likhamanov and Kheisin (1971)	floating freshwater $-30^{o}C$ to $0^{o}C$	dropped ball	1-2400	3-13
Garcia et al. (1985)	freshwater $-5^{o}C$	dropped weight, projectile	1-800	1-20
Kawakami et al. (1983)	freshwater $-8^{o}C$	projectile	2-2000	3-20
	freshwater $-8^{o}C$	projectile fragmentation	20-500	.045
Gerard (1976)	freshwater $-10^{o}C$ to $-1^{o}C$	projectile	250-900	penetration measure only
Yen et al, (1970)	freshwater $-10^{o}C$ to $-1^{o}C$	dropped steel ball	.0025-2.5	only measured coefficients of restitution
Ross (1967)	floating sea and fresh $-8^{o}C$	dropped weight	7-20	.01-.04
Ross (1969)	floating sea ice $-15^{o}C$ to $-4^{o}C$	dropped weight projectile	200-8000	perforation depth only
Comfort and Menon (1981) Glen and Comfort (1983)	sea ice $-25^{o}C$ to $0^{o}C$	dropped weight pendulum	2000-15000	1-3

Table 4.1 (Cont'd.)

Timco and Martin (1979)	floating river ice	dropped weight	2-15	1-5
Brooks (1975)	freshwater	projectile	200-4000	penetration measures only
El-Tahan et al. (1984)	freshwater	dropped weight	120	1.0
McIntosh et al. (1973)	floating sea ice -20^{o} to $-5^{o}C$	air-dropped projectiles	$.05\times10^{6}$ $.25\times10^{6}$	penetration measures only
Young (1973)	floating sea ice	air-dropped projectiles	$.2\times10^{6}$ -15×10^{6}	penetration measures only
Rychnovsky (1987)	floating sea ice	air-dropped projectiles	$.2\times10^{6}$ -1.5×10^{6}	penetration measures only

resistance of the material to impact. If all the energy dissipated during the impact is manifested in the size of the damaged zone, then specific energy is an easily measured and fundamental index. The creation of fracture surfaces is a process that lends itself to measurement in this way since the volume of damaged material can be estimated from the zone where cracking has occurred or from the dimensions of the crater formed. Evidence for ice shows that there is significant energy expended by frictional forces and that the damaged volume depends on the shape of the projectile.

With these points in mind, the results of some ice impact tests are reviewed in this section. Unfortunately, most studies only report penetration depths rather than the volume of damaged material. Given the complexities resulting from the shape of the projectiles, these

results are often specific for given ice and projectile characteristics.

One type of impact test has its origin in weapons testing. Projectiles have been designed to penetrate as far as possible into the ice with minimum resistance or to perforate an ice sheet completely. Tests were performed by Ross (1967, 1969) to evaluate conical and blunt ended projectile shapes for their ability to penetrate sea ice covers in the laboratory and in the field. Very little damage was observed for velocities less than 25 ft/s; some cratering was observed for velocities between 100 and 500 ft/s. At low impact velocities, the blunt end was more efficient; for high impact velocities, a conical end was superior. This is evidence of the rate dependency of ice behaviour.

Other high speed penetration tests have been performed using air-dropped sharp-nosed projectiles (McIntosh et al., 1973; Rychnovsky, 1987). The results of these experiments were penetration depth as a function of impact velocity, with little damage radially from the trajectory.

An interesting study was performed by Gerard (1976), relating projectile penetration on impact to ice crushing strength obtained from uniaxial compression tests on freshwater ice samples. Although the rates of energy dissipation were orders of magnitude apart in these two tests, an approximate power law relation was found between the

results. Given that different mechanisms will act in the two types of testing, the comparison is intuitively weak. The idea of measuring different attributes of an ice sample is, however, a good one.

The above penetration results have been summarised in Figure 4.1. Also included in this figure are the dropped weight results of Timco and Martin (1979), Garcia et al. (1985) and El-Tahan et al. (1984) and the ballistic data from Brooks (1975), Kawakami et al. (1983) and Garcia et al. (1985). The shape and the mass per unit projected area of the projectile are not accounted for in Figure 4.1; this explains in part the scatter in the results. For energies below 10^3 J, penetration depth scaled approximately with the 2/3 power of impact energy. The exponent appears to be less than 2/3 at higher impact energies. Garcia et al. (1985) note that, for cylindrical penetration cavities, the penetration depth should scale linearly with the energy. On the other hand, the volume of open craters should scale linearly with energy and the penetration depth should therefore scale with the 1/3 power of energy as long as the crater shapes are consistent. These hypotheses are not substantiated clearly in Figure 4.1, but the overall trend of the data lies somewhere between the two limits.

Perhaps of more interest in the experimental impact results is the relation between the volume of crushed material and the impact energy. These results are illustrated in Figure 4.2. If the volumetric specific energy were constant, then all results would lie on a 45 degree line of constant specific energy. By noting the sources of the

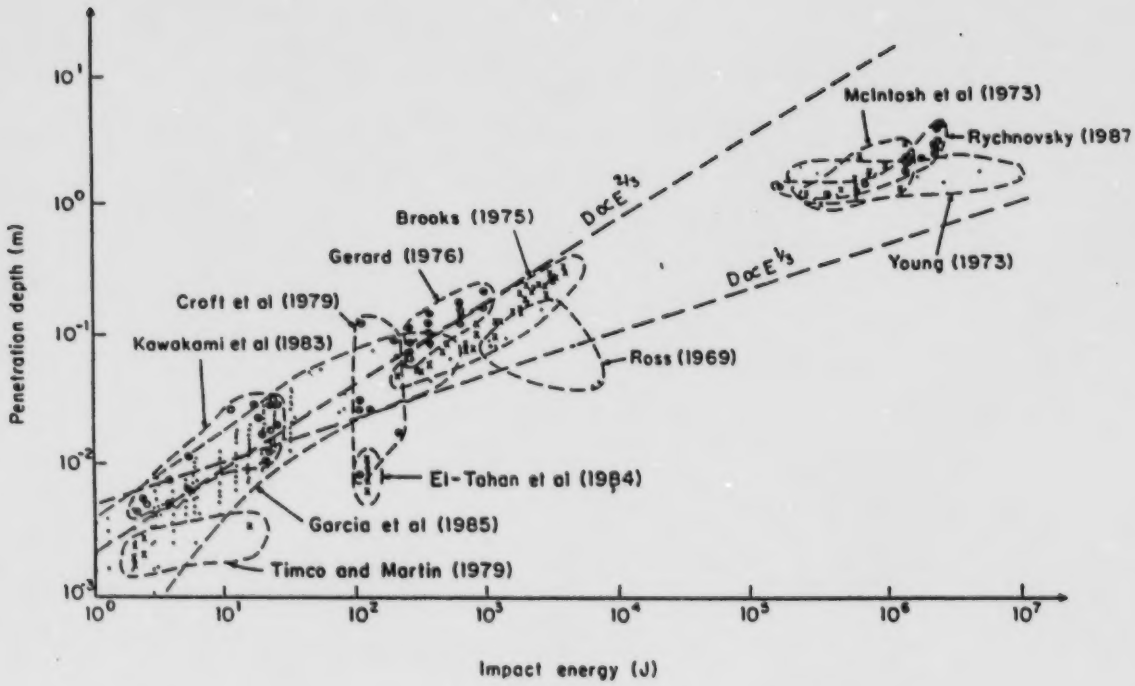

Figure 4.1. Penetration depth vs impact energy for the impact of projectiles on ice from various sources.

different data, a pattern emerges. The lowest specific energies were recorded in the charpy tests by Itagaki and Sabourin (1980) and in the fragmentation tests of Kawakami et al. (1983). There was little or no confinement of the samples, allowing tensile cracks to propagate freely and the crack densities were quite low. In contrast, the bulk samples

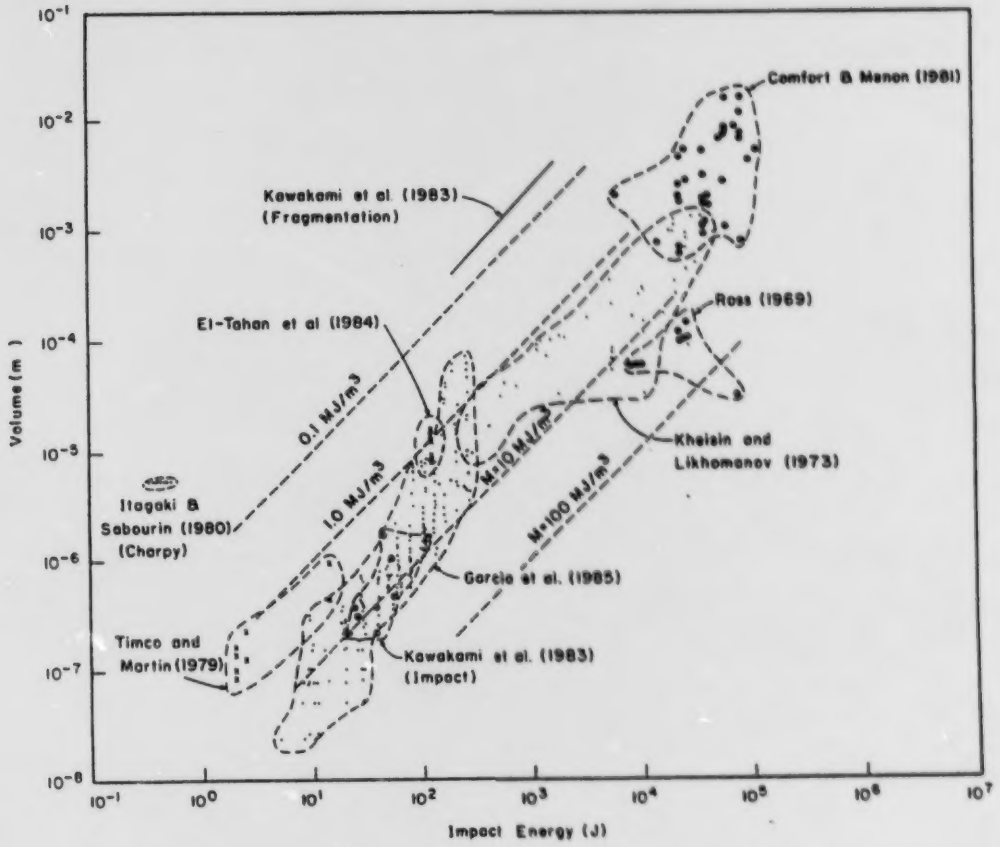

Figure 4.2. Crushed volume vs impact energy for the impact of projectiles on ice from various sources. The dashed lines represent constant values of volumetric specific energy.

and ice sheets used in the other impact tests were well confined, yielding specific energies in the 0.5 MJ/m^3 to 50 MJ/m^3 range. Crack density and pulverised particle size were not very well reported in these tests. Such measurements are fundamental for relating impact energy and fracture energy and might yield some explanations for the range of specific energies reported in Figure 4.2. Confining pressure, believed to inhibit damage and crack formation, should be monitored or better controlled in future impact tests. The ice temperature, the origin of the ice and whether the ice is fixed or floating may also play a large part in the process. Another significant factor is the energy dissipated in friction as the pulverised material is displaced following contact. There was distinct evidence of this in the projectile, dropped weight and pendulum tests described above. The ease with which this material can be displaced is largely dependent on the geometry of the problem. This subject is considered in Chapter 6 of this report.

The failure of specific energy to fully explain impact phenomena has led to the measurement of accelerations and forces during tests. Furthermore, if ice pressures are required for engineering applications, a more direct measurement of forces is preferred over inference from specific energy. Typically, measurements are made using accelerometers placed on the projectile (Ross (1967); Rychnovsky, 1987; Likhomanov and Kheisin, 1971; McIntosh et al. 1973), in the ice (Likhomanov and Kheisin, 1971) and in the frame supporting the ice (Comfort and Menon, 1981; Yen et al., 1970). One advantage of a

projectile-mounted accelerometer is that kinetic energy and displacements can easily be inferred. The deceleration also yields the net resisting force on the projectile. The same direct inference is not possible from accelerometers mounted on the ice or support frame. Particularly for large weights, the stiffness of the support (Comfort and Menon, 1981) has an influence on the recorded accelerations. In this case, the net force was calculated from load measurement pins behind the ice sample and from pressure transducers mounted on the face of the impact weight.

Important results can be obtained from force and acceleration records. First of all, the peak force can be used directly to obtain crushing pressures for design. Decelerations of projectiles can depend on the degree of confinement and the stiffness of the support. Comfort and Menon (1981) also observed the change in pressures over time on the face of the impact weight using pressure transducers. The maximum pressure started at the centre of impact and moved out as the contact area increased. A crushed ice layer was present and was partially extruded during the tests. In penetration tests (Hightower et al. 1982; Young, 1983), peak decelerations did not occur until a significant penetration had taken place. This is in contrast to the results presented by Rychnovsky (1987) in which the peak accelerations appeared early in the penetration.

Average ice resistance pressures on the face of the impact mass have been summarised for various tests in Table 4.2. The tests of El-

Tahan et al. (1984) were done on bulk samples, producing higher impact pressures than those of Likhomanov and Kheisin (1971) that were done on floating lake ice. Comfort and Menon (1981) used saline ice which is inherently weaker and found lower impact pressures. In this last test series, an increase in contact area significantly reduced pressures. Summarising the results of Table 4.2, confinement, flexibility of the support, contact area and ice temperature were found to influence impact pressures.

Although not a direct measure of impact pressure, Timco and Martin (1979) calculated an average impact strength from measured penetration depths and displaced volumes. For small masses of 0.4 kg to 3 kg, average impact strengths of 11 MPa to 15 MPa were calculated for naturally former river ice and 19 MPa to 32 MPa for flooded refrozen ice. These values are high, given that they are averaged over the entire impact, but can be attributed to the small contact areas present.

Little has been done, as yet, to look at the progression of the different mechanisms that take place in the ice as it crushes during an impact test. Kheisin and Cherepanov (1970) describe, in detail, the physical characteristics of the ice cover subsequent to impact by a

Table 4.2 Measured pressures during impact tests, averaged over the impact area. El-Tahan et al. (1984) and Likhomanov and Kheisin (1971) report the maximum pressure for each impact while Comfort and Menon (1981) measured contact areas as the impacts progressed.

Author	Type of ice	Test Conditions	Pressure (MPa)
El-Tahan et al. (1984)	iceberg	60 kg dropped mass, cylindrical shaped ice block -5°C	17
	snow		21
	unconfined snow		17
	S2 fresh		21
Likhomanov and Kheisin (1971)	fresh, lake	156 kg and 300 kg steel balls air temp -30°C - -5°C	12
		+2°C - +4°C	4
Comfort and Menon (1981)	saline 1, 6 ppt	pendulum -25°C, -10°C, -1°C A = 100 cm^2	10
		A = 500 cm^2	2

steel ball. Predominant features were radial cracks and a 2 cm layer of pulverised ice. This pulverised layer was pasty at temperatures near $0^{o}C$ and dry at temperatures of $-20^{o}C$ to $-30^{o}C$. A significant feature was the sharp boundary between the pulverised layer and the adjacent fractured ice.

It is obvious that more fundamental experiments have to be made to improve the understanding of the sequence of mechanisms taking place during impact. The following ideas are suggested:

(i) There is no substitute for a thorough examination of the progression of damage in the ice during impact and of the subsequent state of the ice. It is from this type of observation that pertinent mechanics can be identified.

(ii) The confinement of the ice sample is not the only influence on the size of the damaged zone and the peak pressure. The structural response of the support is also an important influencing factor on the peak loads when the mass of the ice is not significantly greater than that of the impacter.

(iii) The changes in pressure on the face of the indenter were measured by Comfort and Menon (1981) using pressure transducers. This process is still poorly understood. A dense array of pressure measurements throughout the impact is suggested. As an alternative, average pressure measurements

for different geometries of the impacting mass might give some more hints regarding the factors controlling impact pressures.

iv) The influence of friction can be evaluated by measuring the motion of the crushed ice that is expelled from the impact face and the change in the thickness of the crushed layer with time. Further suggestions in this area are made in Section 6.5.

4.3 Indentation Theory

The primary reason for continuous indentation tests is to determine ice forces on ships and fixed offshore structures. The most important quantity to measure is therefore the maximum pressure that the ice can exert. The indentation problem has generally been treated in the literature and in structural design by the approach originally presented by Korzhavin (1962). The force, F, against an indenter is given as

$$F = DhImk\sigma_y, \tag{4.1}$$

where D is the structure width, h is the ice thickness, I is an indentation factor, m is a shape factor (=1, for a rectangular indenter), k is a contact factor (=1, for complete contact) and σ_y is the uniaxial compressive strength of the ice. If the average pressure, p, against the indenter is computed as

$$p = \frac{F}{Dh} \quad , \tag{4.2}$$

then

$$p = Imk\sigma_y . \tag{4.3}$$

The net indentation coefficient can then be expressed as

$$\frac{p}{\sigma_y} = Imk, \tag{4.4}$$

forming the basis of the following arguments.

Various authors (e.g. Michel, 1978; Croasdale et al., 1977) have defined the net indentation coefficient, P/σ_y, for various aspect ratios, D/h, using plasticity solutions. The results of the latter paper are given in Figure 4.3. Some numerical values, calculated from the theoretical elasticity and plasticity solutions described in section 3.3, are given in Table 4.3. In practical situations, the indentation coefficient will lie somewhere between the plane stress solution, p/σ_y=1.15, and the von Mises plane strain solution, p/σ_y=2.97 (equation 3.8), if the plastic assumption is valid. Ralston (1978) disagreed with the above direct application of metal plasticity solutions to ice. His key contribution was in the consideration of different behaviour for tension and compression; the shapes of Ralston's plastic failure criteria were guided by the results of tension, unconfined compression and confined compression experiments on

Table 4.3. Predicted indentation coefficients for a rectangular indenter using plastic solutions.

Yield Condition	Geometry	Indentation Coefficient p/σ_y
rigid plastic Von Mises	plane strain	2.97
rigid plastic Tresca	plane strain	2.57
rigid plastic max. octahedral stress	plane strain	2.42
elastic plastic Tresca	plane stress	1.57
rigid plastic Tresca	plane stress	1.15

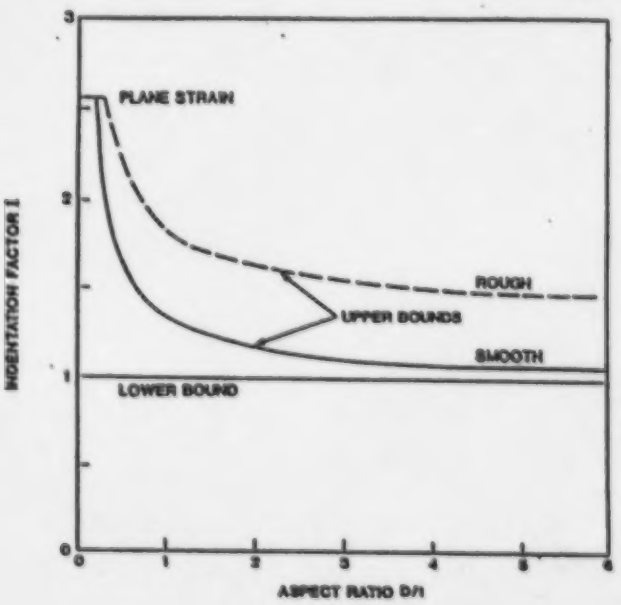

Figure 4.3. Theoretical indentation coefficients (from Croasdale et al., 1977).

ice. From the outline in Sections 2.2 and 2.3, ice is a damaging viscoelastic material and not a plastic material. There is an urgent need to solve the rapid indentation problem considering the influence of progressive damage in the ice.

4.4 Indentation Experiments on Ice Sheets

Many indentation tests have been carried out for ice sheets in order to obtain design values for the indentation coefficient (e.g. Neill, 1976). These are summarised in Table 4.4. Since brittle failure mechanisms in compression are the focus of this review, emphasis is placed on tests in which evidence of crushing, clearing and spalling is present. Energy input to the ice is not generally controlled in these tests; the speed of the indenter is held constant and the energy varies with the force required to drive it.

A controlling factor on the dissipation of energy during brittle compressive failure is the degree to which the ice is confined. This determines the volume of ice over which failure takes place. In the continuous indentation of ice sheets, the measure used to represent confinement is the aspect ratio of the indenter width to the ice sheet thickness. In the studies of Table 4.4, maximum pressure was found to decrease as a function of aspect ratio. In the brittle range, maximum pressure also decreased slightly with increasing indentation speed. The velocity influence was most prominent at aspect ratios below about 2.5 (e.g. Sodhi and Morris, 1984) but not significant above this value.

Table 4.4. Summary of continuous indentation tests on ice sheets in the brittle failure range

Authors	Ice Conditions	Aspect Ratio Shape of Indenter	Velocity (ms^{-1})	Indentation Coefficient
Sodhi and Morris (1984)	urea doped -1°C	1-10 rectangular	.01-.2	8-2
Sodhi and Morris (1986)				
Timco (1986)	fresh -3°C	1-25 rectangular	.001-.6	2-0.3
Timco and Jordaan (1987)				
Michel and Blanchet (1983)	fresh 0°C	0.5-83 rectangular	.07	3-1
Tsuchiya et al. (1985)	saline -3.5°C	1.5	.005-.06	5-2.5
Bohon and Weingarten (1985) Bohon (1984)	fresh -10°C	.25-4.5 cylindrical	.005	3-1
Evans et al. (1984)	fresh -10°C	2	.002-.05	-
Kry et al. (1978) Kry (1979a, 1979b)	fresh -10°C, -2°C	2.5-20 cylindrical	.005-.25	-
Hirayama et al. (1974)	fresh 0°C	0.5-5 cylindrical	.00004-.012	5-1.5
Zabilansky et al. (1975)	fresh -3°C	0.4-30 rectangular, cylindrical	.001-.7	-

The results of Timco (1986) did not show much velocity effect over the range of nominal strain rate V/2D of 2×10^{-2} to 10^{1} s^{-1}. The evidence of a velocity dependence on peak pressures in the brittle range is

still not conclusive.

The choice of peak pressure as the force measure is essential from a design perspective. Michel and Blanchet (1983) found, in some cases, that the pressure was highest at the start of the test on the intact ice sheet. This is not surprising; it may be the result of full contact or the result of different failure mechanisms present. The idea of Kry (1978) to consider the statistical distribution of forces is realistic; it does not, however, resolve the fundamental mechanisms associated with the different ice pressures.

The influence of the strain rate on the uniaxial compressive strength is generally ignored in the application of Korzhavin's equation to fast indentation tests (e.g. Sodhi and Morris, 1984; Michel and Blanchet, 1983; Bohon and Weingarten, 1985; Tsuchiya et al., 1985; Timco, 1986). This is justified since no systematic rate dependence has been found in fast uniaxial tests (e.g. El-Tahan et al., 1984). There are complications when comparing the rate at which the indentation and uniaxial compression tests are carried out. Recalling equation (3.9), an equivalent strain rate, $\dot{\epsilon} = V/\alpha D$, has been assumed where α is a constant, V is the speed and D is the width of the indenter. Michel and Toussaint (1977) postulated $\alpha=4$ from an argument based on rigid plastic failure in plane strain and Ralston (1979) recommended the selection of $\alpha=2$. The length scale, αD, should truly be the distance over which the deformation takes place. Jordaan and Timco (1987) have estimated that most of the crushing energy is

expended in the thin crushed layer immediately adjacent to the indenter, shown schematically in Figure 4.4. Should not the strain rate used for indentation then reflect the crushed layer thickness? It is certainly much less than 4D or 2D.

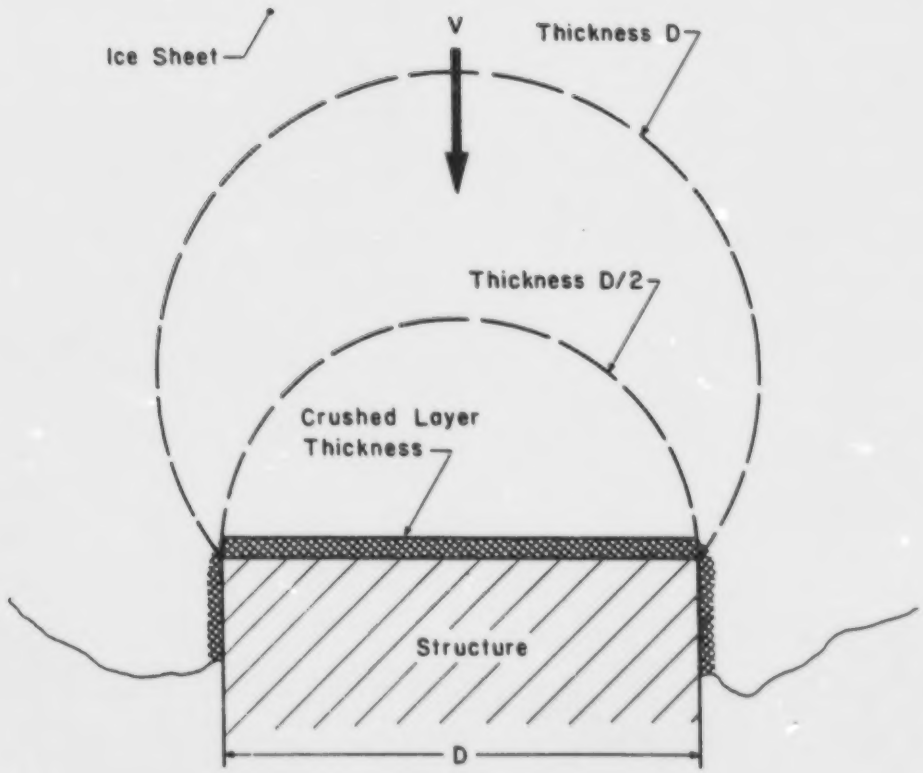

Figure 4.4. Continuous indentation of a rectangular indenter showing the crushed layer.

The indentation coefficient is illustrated as a function of aspect ratio for Timco (1986) and Michel and Blanchet (1983) in Figure 4.5. The values ranged from 0.25 to 2.0 for Timco (1986) and 0.75 to 3.25 for Michel and Blanchet (1983). For a cylindrical indenter, Bohon and Weingarten (1985) calculated a range of indentation coefficient from 3 to 1 for similar aspect ratios.

Ralston's (1978) plastic solutions for the indentation problem gave indentation coefficients that varied from about 3 for the plane stress case to 4 in plane strain. These values of the indentation coefficient exceed those in the above experiments. While the experimental values are perhaps closer to the plastic values given in Table 4.3, the comparison is less appropriate. The plastic solutions should not be reduced to fit the data of Figure 4.5 using the contact factor in equation (4.1); the development of a plastic failure zone should not depend on the degree of contact at the laboratory scale. The contact factor should only be used, as it was intended, for scaling between laboratory and field conditions. It appears from these indentation test results that brittle failure processes took place during the indentation resulting in lower loads than the plastic theory would indicate.

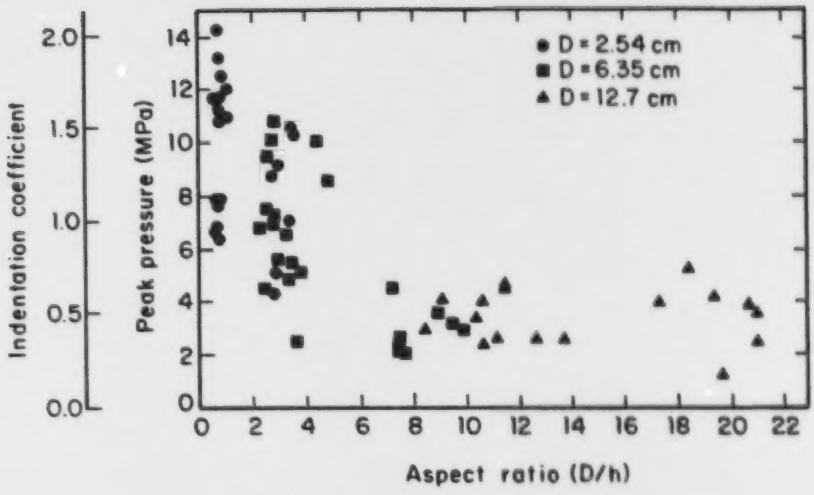

(a)

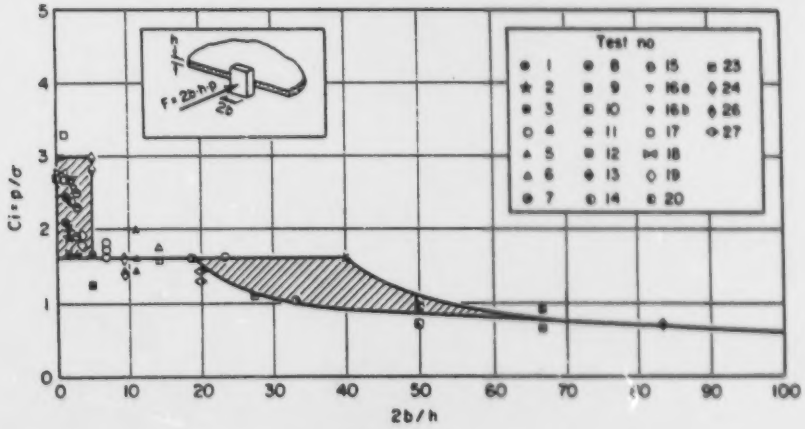

(b)

Figure 4.5. Indentation coefficient, p/σ_y, as a function of aspect ratio, D/h. (a) shows the results of Timco (1986) and (b) gives the values found by Michel and Blanchet (1983).

The indenter force vs time trace has some characteristic patterns from test to test (e.g. Michel and Blanchet, 1983; Evans et al., 1984; Sodhi and Morris, 1984; Määttänen, 1983; Timco and Jordaan, 1987). The traces are oscillatory with relatively consistent maximum and minimum values. There is some evidence that the applied force at constant velocity is largest for the first peak corresponding to a uniform contact at the face of the indenter. All of the above tests show a characteristic "sawtooth" pattern; a gradual rise in the force is followed by a sharp drop, as illustrated in Figure 4.6. An assessment of this repeated pattern will be made in Chapters 5 and 6 of this report.

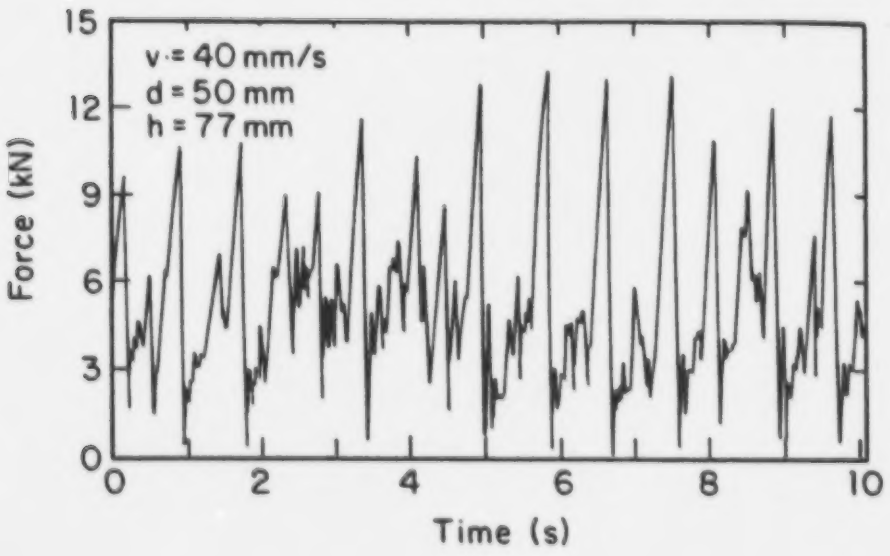

Figure 4.6. Oscillating force during continuous indentation showing "sawtooth" pattern (from Sodhi and Morris, 1984)

Thus far, little attempt has been made to analyse the frequency of the load oscillations caused by ice crushing. MÄättÄnen (1983) has extensively studied the oscillations of flexible structures, but has ignored the periodic nature of the ice failure process itself. Sodhi and Morris (1986) looked at the oscillations in urea-doped ice and found an increase in characteristic frequency with the speed of indentation and a less significant decrease with aspect ratio. They also related the mean size of the damaged zone to the ice thickness. Their value for the ratio of damage zone length to ice thickness of 0.4 is similar to the value obtained by Neill (1976). Timco and Jordaan (1987) directly measured the size distribution of ejected particles and found a good correlation with the dominant observed frequency. For flexible structures, Tsuchiya et al. (1985) report an increase in the dominant frequency with indentation rate up to a given "natural ice frequency".

There is a tendency to ignore the actual mechanisms involved when calculating maximum ice pressures. Without this, no real understanding of the process can be made. The two fundamental variables that influence the failure mechanism and the resulting indentation pressures are the speed of the test and the confinement (represented by the aspect ratio). The results of Timco (1986) and Evans et al. (1984) are reproduced in Figures 4.7 and 4.8 respectively. Similar conclusions were reached by Michel and Blanchet (1983). An important feature to note is the combination of crack formation, spalling and crushing under different test conditions; seldom is one mechanism found alone.

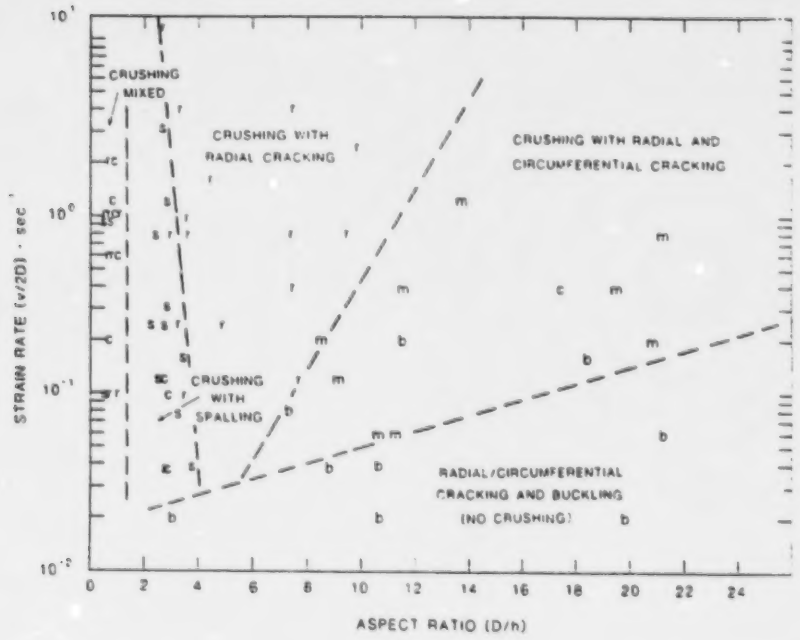
CRUSHING MIXED
CRUSHING WITH RADIAL CRACKING
CRUSHING WITH RADIAL AND CIRCUMFERENTIAL CRACKING
CRUSHING WITH SPALLING
RADIAL/CIRCUMFERENTIAL CRACKING AND BUCKLING (NO CRUSHING)
STRAIN RATE (v/2D) - sec⁻¹
ASPECT RATIO (D/h)

Figure 4.7. Map of brittle failure mechanisms for ice in continuous indentation as a function of rate and aspect ratio (from Timco, 1986).

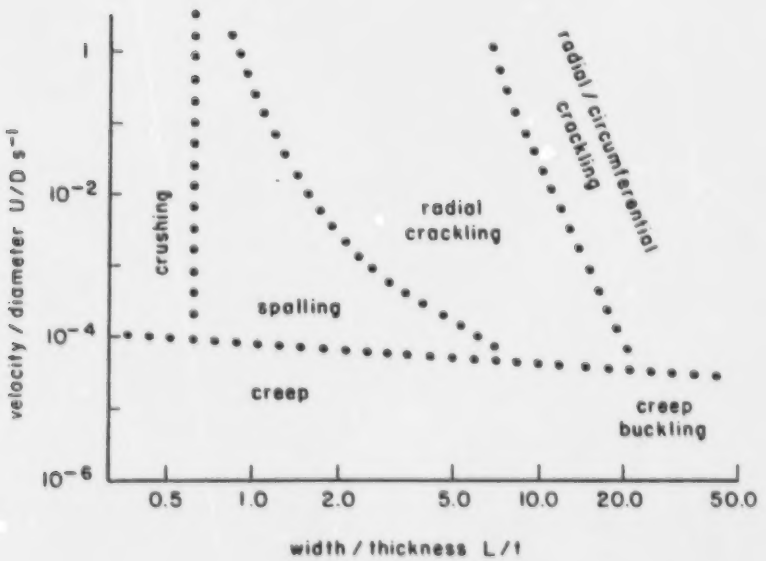

Figure 4.8. Map of failure mechanisms for ice in continuous indentation as a function of rate and aspect ratio (from Evans et al., 1984).

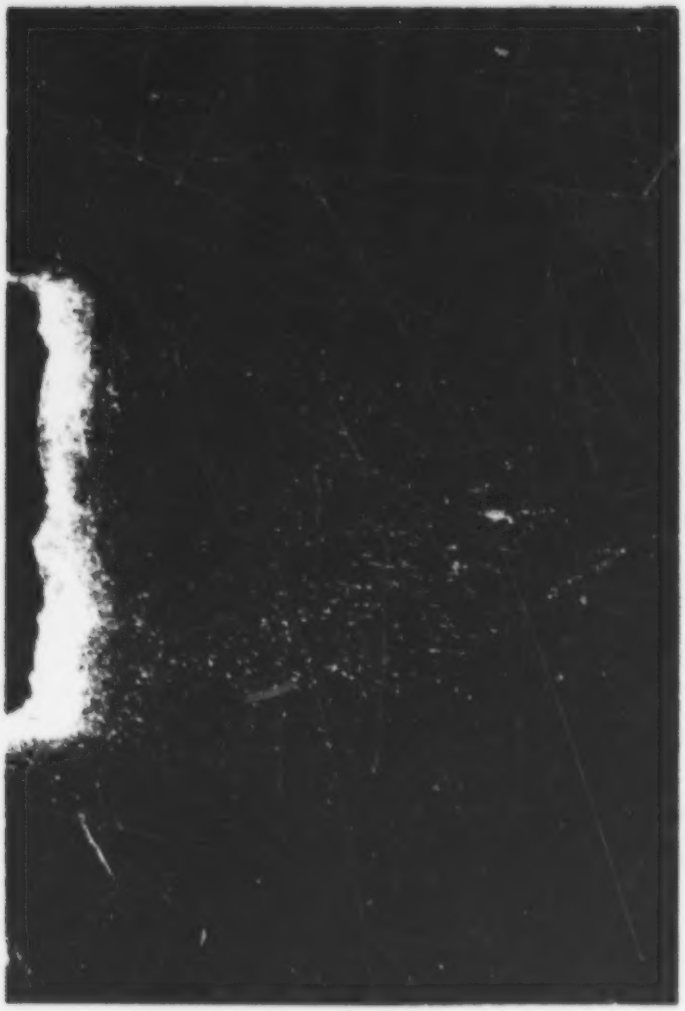

Figure 4.9 Microcracking against the face of an indenter during a continuous indentation experiment. The indenter width was about 6 cm.

Crushing is predominant under a high degree of confinement and faster indentation velocities (e.g. Figure 4.9). Note the thin layer of pulverized ice adjacent to the face of the indenter and the systematic progression of cracks. Comparison with the Michell elastic solution, (e.g. Timoshenko and Goodier, 1970), shows that the cracks are formed along lines of maximum shear. The concept of shear damage is discussed further in section 5.3.

4.5 Continuous Indentation of Bulk Samples

In the continuous indentation of bulk samples, the indenter is typically applied to the surface of an ice block at a given rate and the required force is measured. Confining pressures are higher than in ice sheet indentation; ice samples are usually granular and more representative of iceberg ice.

Mobil conducted an experiment at Pond Inlet using a spherical indenter in tunnels carved out of a grounded iceberg. Johnson and Benoit (1987) have published the pressure-area relation that resulted from this study; it is reproduced here in Figure 4.10.

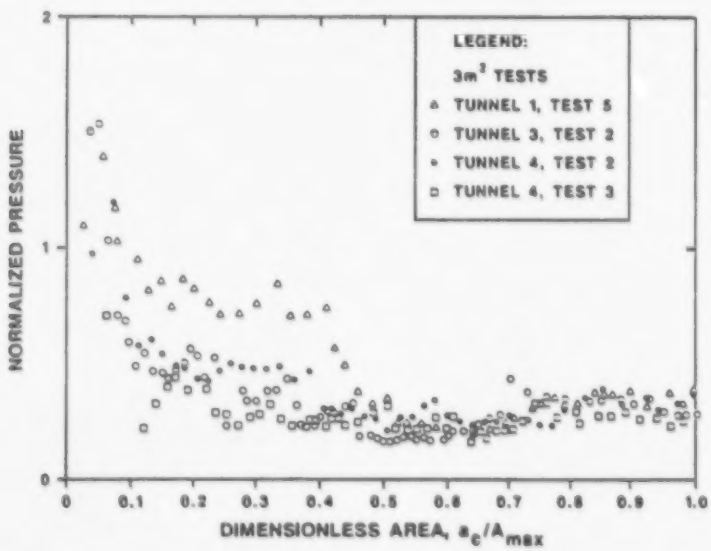

Figure 4.10 Pressure-area relation from Mobil's spherical indenter tests at Pond Inlet (from Johnson and Benoit, 1987). The areas have been normalised by $A_{max} = 3\ m^2$ and the pressures by lab measurements of the uniaxial strength of the ice.

If the uniaxial strength of iceberg ice is about 7 MPa (e.g. El-Tahan et al., 1984), then average pressures over this area were approximately 2 MPa for areas greater than 1.5 m^2.

Nadreau (1987, unpublished) used a smaller spherical indenter on multi-year ice. The preliminary indication from these tests is that a "sawtooth" like oscillation pattern was observed (see Jordaan et al., 1987) and that a significant amount of pulverised ice was extruded from the face of the indenter.

Laboratory experiments on bulk samples have been reported by El-Tahan et al. (1984) and Garcia et al. (1985). For circular and cylindrical indenters of areas less than 1600 mm^2, El-Tahan (1984) reported peak pressures of 15 to 30 MPa. Garcia et al. (1985) found peak pressures of up to 35 MPa to be relatively insensitive to the indentation rate for areas less than 300 mm^2. In this last study, energy input as a function of penetration rate was similar to that obtained in impact tests by the same authors.

The above tests illustrate a scale effect for indentation pressures. When brittle mechanisms are present, there is a significant decrease in applied pressure with the area of the indenter for areas up to about 1.5 m^2. As yet, it is not known whether there is a decrease in pressure for areas larger than 3 m^2.

5. DAMAGE PROCESSES IN ICE

5.1 Role of Damage Mechanics

In the analysis of stresses and strains in a continuum, the following ingredients are needed in any formulation:

(i) A statement of equilibrium, static or dynamic;

(ii) A statement of compatibility; the pieces fit together; and

(iii) The connection between (i) and (ii), that is, the constitutive equations of the material.

The situation in fast impacts between ice and a structure is illustrated in Figure 5.1 - large tensile and flexural cracks may also complicate the picture, but these are omitted since the focus of the present work is on the crushing of ice.

Crushing describes the pulverisation of ice in predominantly macroscopically compressive fields of stress, by the joining together of myriads of cracks so that the crushed ice particles to move as separate entities. Eventually, they no longer form a solid continuum and behave more as a viscous fluid (Kheisin and Likhomanov, 1973; Kurdyumov and Kheisin, 1976; Likhomanov and Kheisin, 1971). The process of transformation of the virgin ice to a powder can be appreciated quite vividly by contrasting the final crushed ice with the initial solid ice mass. This process is one of progressive damage.

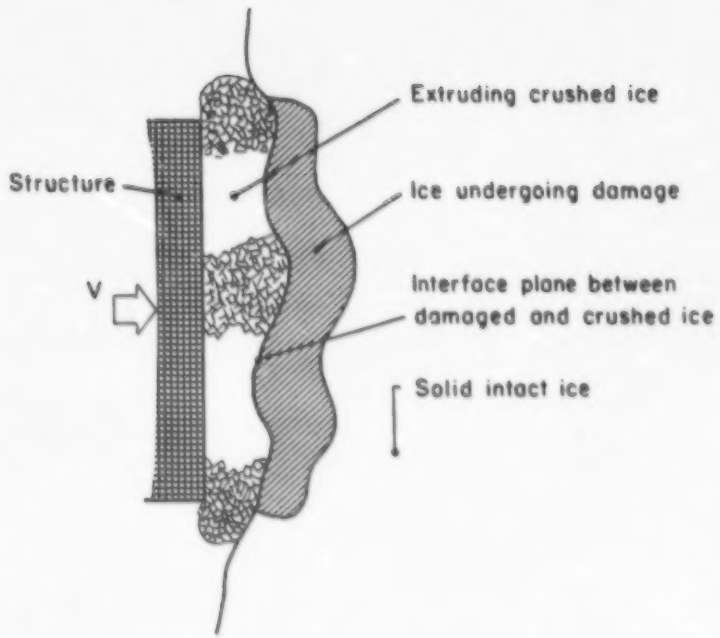

Figure 5.1. Illustration of crushing of ice between solid ice and a structure.

In order to implement the program suggested by the steps (i) to (iii) above, it is necessary to idealise the ice in a way that recognizes its spatially varying constitutive behaviour - from an intact solid to a powder. There is no way of obtaining the force distribution and hence the force unless one resorts to empirical means (this is not to decry the latter: nevertheless it is preferable if empirical methods are developed along with theory).

A further complication is that the situation is likely to be dynamic. Figure 5.2 illustrates the form of the force-time relationship that has been observed to result from continuous movement of ice against a structure, at rates high enough to cause crushing. If a material is indented, and undergoes creep or plastic flow, a smooth force-time curve will result. The occurrence of repeated pulverisation and clearing, resulting in a dramatic oscillation in load, is related to the brittleness. The importance of taking these effects into account in design is illustrated by the response of the Molikpaq structure in moving ice (Jefferies and Wright, 1987).

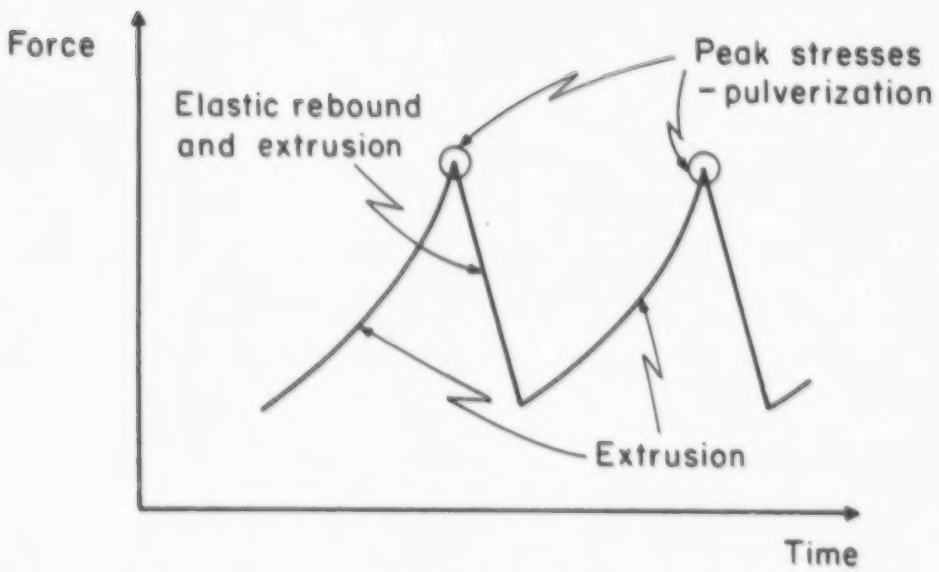

Figure 5.2. Dynamic force-time relationship and ice crushing.

As illustrated in Figures 5.1 and 5.2, it is suggested that the peak load depends on the disintegration process of the ice - hence the importance of damage mechanics. Nevertheless, the load is often transmitted through a layer of crushed ice, so that this has to be included in the analysis. If it is accepted that analysis of the crushed ice is a "flow" problem, then the analysis becomes complicated by the fact that usually one part (the solid mechanics part) will be analysed with Lagrangian coordinates whereas the "flow" part is generally analysed using the Eulerian system (see also Jordaan, 1986). In the present review, the damaging ice is considered in the following sections and the flow of crushed ice is dealt with in Chapter 6. The analyses should nevertheless be seen as part of the same problem, and have to be linked in some manner. A final complication should be mentioned: the thickness of the layer of crushed ice will certainly vary, possibly in a systematic way, but also with some "statistical" variations. This aspect should also be investigated.

Having recognized some of the difficulties inherent in the analysis of ice crushing and clearing, it is important to develop a strategy whereby fundamental understanding will improve but at the same time practical objectives of obtaining design formulations are met. A good appreciation of this has been presented by Riska and Frederking (1987). The fact that the damaging ice is subjected to a state of triaxial compression is addressed and failure surfaces are developed based on the results of triaxial tests. The brittle failure at high strain rates results in a failure surface, distinguished from a yield

surface at lower strain rates. The penetration process was addressed using an empirical pressure-area relationship proposed earlier by Varsta (1983) for ice loads on ships.

A reasonable approach therefore seems to consist of analyses carried out at various levels in a consistent manner; a damage mechanics model need not contain all details of crack densities, lengths and orientations yet should be capable of being adjusted to account for this information. For instance the parameter measuring the extent of damage might be responsive to microstructural information of the kind just noted.

5.2 The Damage Process

The heterogeneous structure of many materials includes dislocations, grain boundaries, microcracks and voids. These propagate and develop under compressive stresses. The propagation of large cracks in tension is not the concern of the present analysis. Rather, the system of microcracks that develop under compressive stresses is the subject of the present discussion. One of the first studies of crack development with time in ice under compressive states of stress was conducted by Gold (1972).

Consider a specimen of material, such as concrete, rock, or as we have seen ice, loaded in compression. If one subjects the material to a small increment of stress or strain, there can be several effects on

the material. There may be an increase or decrease in elastic strain energy; there may be irreversible movements associated with creep or plastic flow; last, the microcrack system may extend and new microcracks could be nucleated: this is the essence of the damage process. Generally, the crack growth will be stable so that damage increases in a relatively orderly manner.

It is important to recognize that elasticity, creep or plastic flow do not of themselves result in material damage or degradation. Storage of elastic strain energy is a reversible process without any effect on the structure of the material. On the other hand, creep and plastic flow are irreversible (involving heat generation); nonetheless the structure of the material is restored after the movement of dislocations.

The mechanism for the progress of damage above involves changes to the structure of the material; as the density and size of cracks increases, the response of a specimen of macroscopic size changes. Figure 5.3 shows the changes in the stress-strain curve for concrete under successive load cycles. This phenomenon is exhibited by many materials with a strain-softening descending branch, and one such material is ice. The damage can occur at a fast rate, without substantial time-dependent response of the ice, or slowly, leading to a gradual development of damage with time. In this case, the damage is referred to as creep damage (Leckie and Hayhurst, 1974; Leckie, 1978)

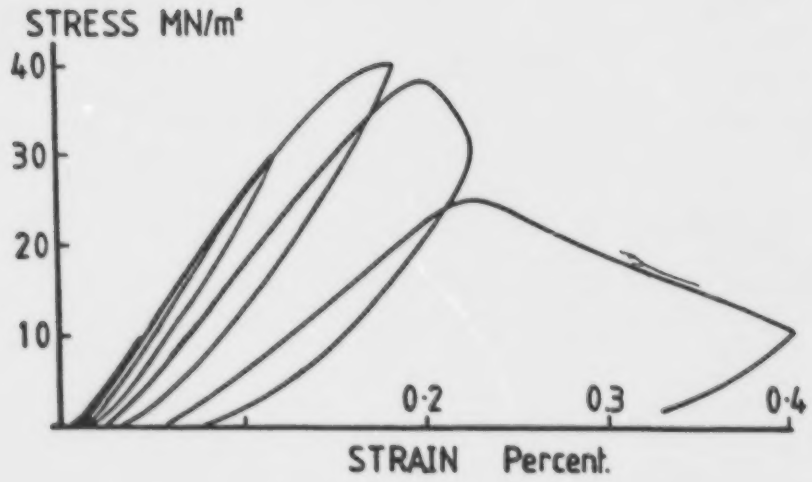

Figure 5.3. Cycle loading of concrete in compression based on the work of Spooner and Dougill (1975).

although the resulting change to the material is damage, not creep (which occurs simultaneously).

5.3 Cracks in Compression

In Figure 4.9, a dense array of cracks can be observed, with the extent of cracking increasing as the indenter face is approached. Following on from the four points summarised at the end of Chapter 3, cracks in the compressive field near the indenter or structure are considered. The suggestion that the cracks might be shear (mode II) cracks (Jordaan, 1987) met with the expected expressions of horror from some members of the fracture mechanics community. In uniaxial compression, cracks often align in the direction of stress, possibly

resulting in failure by "slabbing". No doubt, these become less prominent when the piece of ice is under triaxial compression. Why should cracks not initiate and propagate in shear? They certainly propagate along lines of maximum shear (Figure 4.9), and do not resemble wing cracks (Ashby and Hallam, 1986). These aspects deserve further study.

There is no doubt that cracks exist in compressive states; the possible mechanisms of energy dissipation are illustrated in Figure 5.4. Dissipation of energy can take place by the following mechanisms

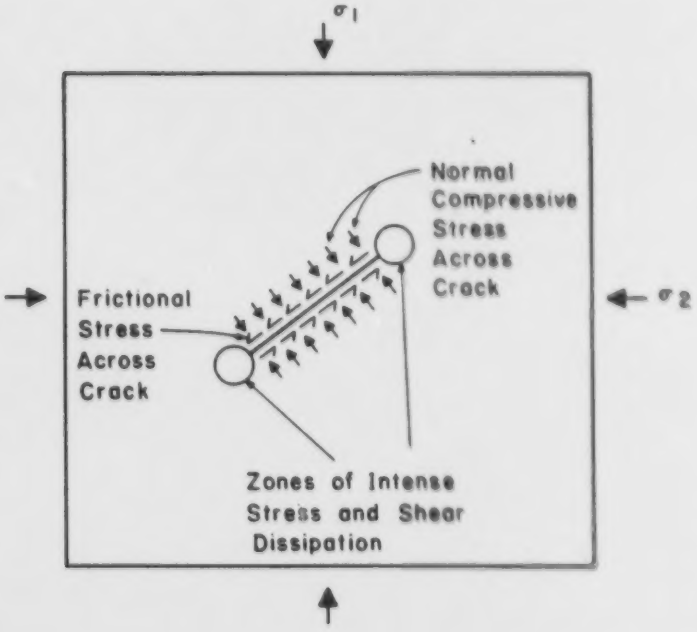

Figure 5.4. Crack in compression.

if an existing crack responds to a shear across it by distorting it further:

(i) Dissipation by creep in the zones near the crack tip; note that creep is dependent on stress to the third power and that stresses are intense.

(ii) Friction across the crack surfaces. When crack coalescence takes place and the particles move relative to each other, this mechanism becomes the chief dissipator of energy.

These mechanisms do not necessarily involve extension of the crack itself and may well explain the apparent cessation and stabilisation of damage followed by dissipation without further damage, as exhibited in Figure 2.7. (Note that this will only happen if the energy input is kept under control).

Further fundamental study in the above areas would aid our understanding of the processes involved.

5.4 Continuum Damage Mechanics

To follow each crack in the analysis of the material would very, soon result in an undersirable degree of complexity, and indeed an undesirable degree of detail. In damage mechanics, the effect of the growing network of cracks is "smeared" out so that the effect on

continuum properties, appropriately averaged, is taken into account in the analysis. The rationale for this is sensible because the number of cracks is large; repetitive tests on similar specimens would yield quite different detailed crack patterns, though with similar "average" behaviour.

The literature on damage mechanics, from the point of view of material modelling, is wide. A review of continuum damage mechanics has been conducted recently by Krajcinovic (1984) and this provides an excellent starting point. It must be emphasised that almost all of the work in the area of damage mechanics has been computer-oriented, using for example finite element analysis. It is important in the future to develop closed form techniques.

In continuum damage mechanics, the material damage is distributed uniformly in the volume (possibly small) of material under consideration. The damage results in a degradation of elastic properties. A simple bilinear stress-strain relationship is shown in Figure 5.5. It is important to note the change in elastic modulus after the onset of degradation, typified by the change in slope of the unloading curve, as illustrated in Figure 5.6. More sophisticated relationships are shown in Figure 5.6; it is important to note that, after a certain amount of damage, the material is unlikely to have memory of the origin so that unloading curves of kind illustrated in Figure 5.6(b) are more realistic. In order that the damage illustrated in Figures 5.5 and 5.6 can develop in a progressive fashion, the tests

would be conducted with control of the incoming mechanical energy, for instance in a strain-controlled test. Various measures of damage have been proposed: generally they relate to the change of elastic modulus. The increasing network of cracks (damage) results in the formation of stress-free zones or voids, thereby causing higher effective stresses in the undamaged material. Lemaitre and Chaboche (1978) use this concept to relate the elastic modulus to the true contact area. The "effective" elastic modulus, i.e. averaged over the damaged and undamaged zones, is reduced. For the remainder of this section, the material will be considered elastic, although allowance can be made for work (creep or plastic) at small zones near the crack tip.

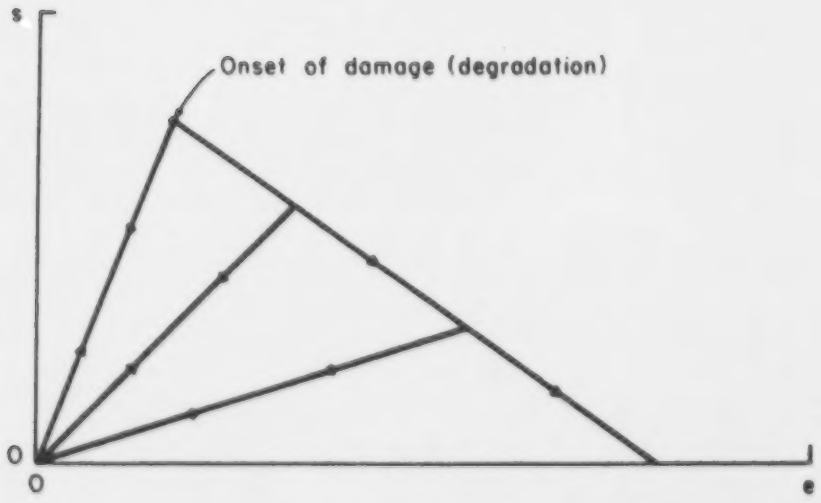

Figure 5.5. Simplified bilnear damage model.

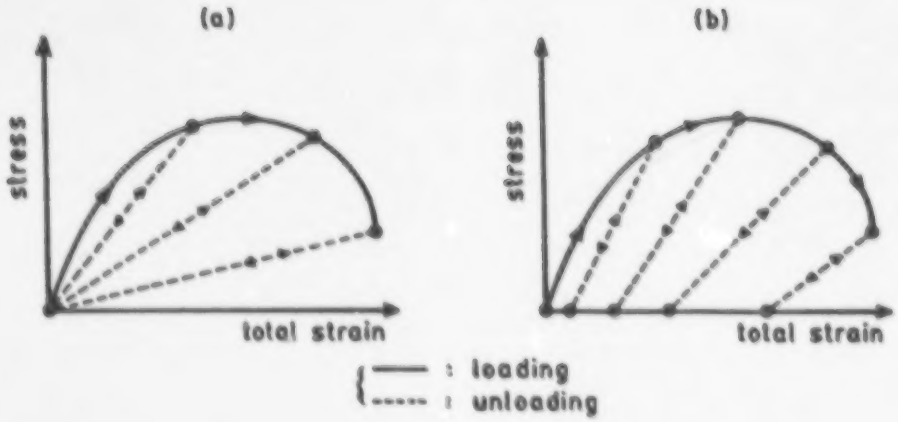

Figure 5.6. Damage relationships: (a) with memory and (b) without memory of origin.

A formulation of damage evaluation for elastic bodies has been given by Dougill in a series of papers (Dougill 1983a, 1983b, 1975, 1976; Dougill et al. 1976; Dougill and Rida, 1980). The formulation starts with the generalized Hooke's law,

$$\sigma_{ij} = C_{ijkm}\,\epsilon_{km}, \tag{5.1}$$

and deals with materials of the kind illustrated in Figure 5.6(a). This can be differentiated with respect to time (denoted by superimposed dots) to give

$$\dot{s}_{ij} = C_{ijkm}\,\dot{\epsilon}_{km} + \dot{C}_{ijkm}\,\epsilon_{km}. \qquad (5.2)$$

Although the effects related to the two terms on the right of equation (5.2) occur during the same time interval, it is useful to consider them separately. The first is the elastic component (as if there was no degradation); the second is related to the change in stiffness (modulus) of the material and was termed by Dougill the fracture stress decrement. Dougill developed a theory analogous to hardening plasticity, but with the use of Il'ilushin's postulate. These theories will not be pursued here; rather, a relatively tractable approach suggested by Resende and Martin (1983a, 1983b, 1984) will be described. In this, we consider only shear damage, omitting the dilational terms developed by Resende and Martin.

The deviatoric components of the stress and strain tensors are written as

$$s_{ij} = \sigma_{ij} - \frac{1}{3}\,\sigma_{kk}\,\delta_{ij}$$

and $$e_{ij} = \epsilon_{ij} - \frac{1}{3}\,\epsilon_{kk}\,\delta_{ij}$$

respectively, where δ_{ij} is the Kronecker delta. We consider now the effective shear stress s as

$$s = (\tfrac{1}{2}\,s_{ij}\,s_{ij})^{1/2} \qquad (5.3)$$

which is invariant, and can be thought of as a constant times the root mean square of the maximum shear stresses. The model considers the damage to be represented by the parameter λ, with $0 \leq \lambda \leq 1$; $\lambda=0$ represents "no damage" while $\lambda=1$ represents "total failure" and loss of shear stiffness. Formally, the value of λ decides the value of the shear modulus, i.e.

$$s = Ge = G_o(1-\lambda)e \tag{5.4}$$

where G_o = initial shear modulus. From (5.4):

$$G = G_o(1-\lambda) \tag{5.5}$$

and it is possible to derive the following rate forms of (5.4):

$$\dot{s} = G_o(1-\lambda)\dot{e} - G_o e\dot{\lambda}, \text{ for loading } (\dot{\lambda}>0)$$

$$\text{and } \dot{s} = G_o(1-\lambda)\dot{e} \text{ for unloading } (\dot{\lambda}=0) \tag{5.6}$$

It is important to note that unloading does not involve any progressive damage and that the model, in the structure of equations (5.4) to (5.6) embodies the assumption that the material returns to the origin (e=0) on unloading.

The summary above is intended to provide an overview of the

direction of theoretical work that the writers feel to be potentially fruitful in the study of the pulverisation of ice. One application along the lines of the theory above has been conducted by Cormeau, Jordaan and Maes (1986). This included also the consideration of residual strains on unloading (loss of memory).

Further development of damage mechanics is necessary to the understanding of the crushing off ice. The work of Resende and Martin suggests that the damage rate $\dot{\lambda}$ be considered as a function of $\dot{e}$, e and p (= 1/3 σ_{ii}). In line with the reasoning in the present paper, it is proposed to consider

$$\dot{\lambda} = \dot{\lambda}\ (W,E), \tag{5.7}$$

where E is internal energy and $\dot{W}$ = dW/dt is the rate of work done on a unit volume by the surroundings. Clearly if $\dot{W}<0$ then $\dot{\lambda}=0$ (unloading) and for $\dot{W}>0$ there is energy available for the creation of new surfaces. A theory along these lines is being developed by the authors, taking into account the initiation of new cracks as well as the propagation of existing cracks; the densities and lengths are of importance.

In the above, a scalar damage function has been considered; this is an appropriate simplified starting point for the theory. Krajcinovic (1984) makes a good case for a vectorial representation. In the case of ice, the shear damage could be anisotropic and this would require directional information. Recently, Sjolind (1987)

calibrated a continuum damage model to mechanical parameters for ice obtained from Michel (1978). This vector damage model is similar in form to that of Krajcinovic and Fonseka (1981) and is in fact identical for the uniaxial test cases presented in Fonseka and Krajcinovic (1981).

Two other aspects deserve attention: the effect of concurrent hydrostatic confining pressure on the damage process as well as the dilalational effects associated with this process. Above all, further experimental work is needed to study the damage process and to determine material parameters. The relationship of damage to flow is illustrated in Figure 5.7.

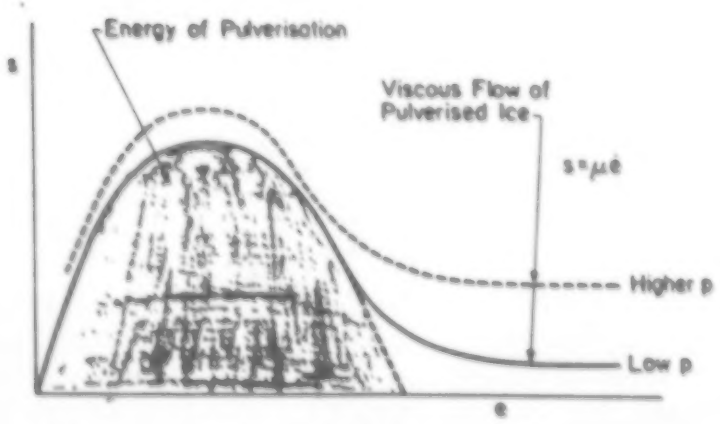

Figure 5.7. Energy of pulverisation and subsequent flow of crushed ice. The graph shows the hypothetical effect of hydrostatic pressure, p.

5.5 Non-Uniqueness of Stress-Strain Relationships

In the theories of elasticity and plasticity it is common to draw stress-strain curves and to treat them as "fixed". On the other hand, it is not difficult to contrive creep tests in which different stress-strain curves are obtained.

In damage mechanics, some authors have used fixed stress-strain relationships. This may be a reasonable approximation in some cases, but it is true that the stress-strain relationship is affected by the energy entering the specimen.

As a first example, consider the dependence of the stress-strain relationship on the testing method. Two standard tests are shown in Figure 5.8. The test method has long been known to affect the result; for instance flexible test machines with load control can feed strain energy into a specimen that is beginning to be damaged, enhancing the rate of damage and possibly resulting in a sudden unstable failure.

At a given point on the stress-strain curve, once damage has commenced, there will be a certain density of cracks with a distribution of crack lengths. The addition of a small amount of energy to the specimen will result in an increase in the damage, and for elastic response of the material, it is possible to have a given (unique) amount of damage for a certain change in strain (the energy

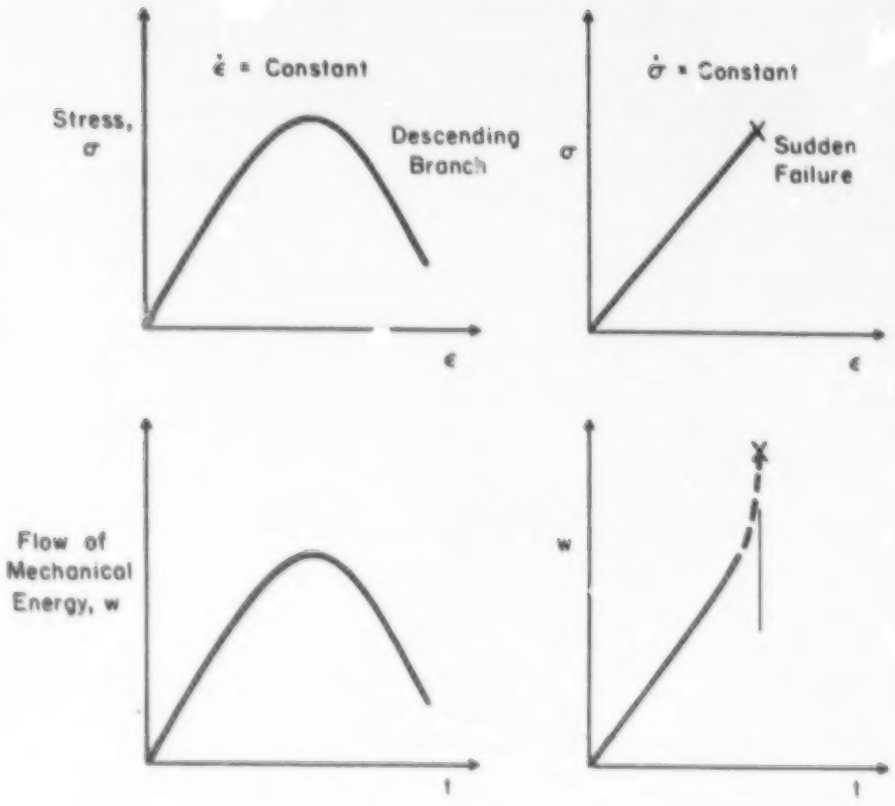

Figure 5.8. Strain and stress controlled tests and associated flow of mechanical energy into the specimen.

input being given by stress multiplied by change in strain). Thus a unique stress-strain curve results.

In the preceding discussion, frictional dissipation across the crack faces has been ignored. It has been noted that ice exhibits a stabilization of damage under controlled conditions (Figure 2.7); a

certain amount of damage occurs and then the process halts. Energy continues to be dissipated at a constant rate, and mechanisms for this dissipation have been suggested (Figure 5.4), involving essentially frictional processes. If this is accepted then the addition of a small amount of energy can result in this energy being spent on dissipation and further damage. A large number of possible stress-strain curves exist, depending on the rate at which energy is added and the current state of damage. Figure 5.9 shows the range of stress-strain curves that can be attained by the control of energy entering the specimen.

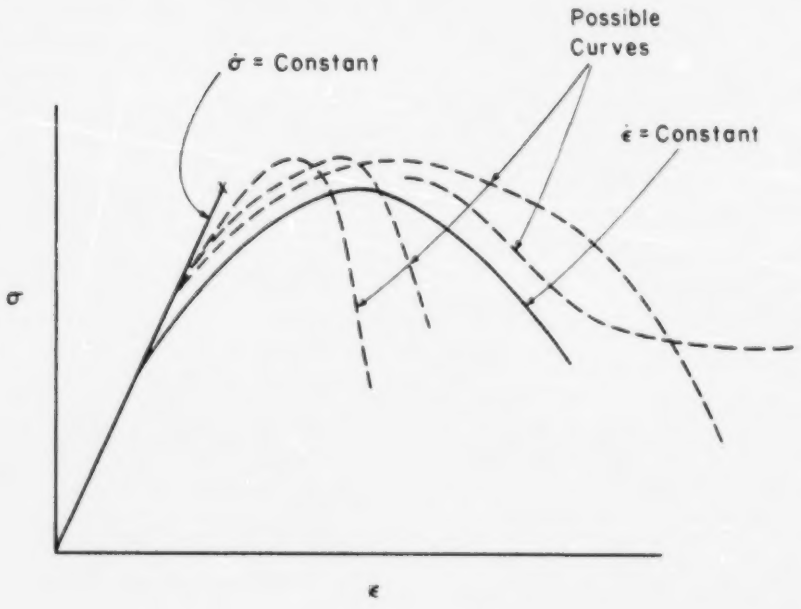

Figure 5.9. Non-uniqueness of stress-strain relationship for damaging materials.

To the writers' knowledge, no systematic study of damage has been completed with the question of energy fluxes being considered as a basic aspect. It seems that this should be considered especially in planning experimental work and in setting up models of material behaviour.

5.6. Energy Effects.

Some important ideas relating to the energy dissipated during crushing can be drawn from the analysis of ice impact and indentation in Chapter 4. While a significant amount of energy went into the removal of pulverised material, there was also a finite energy that could be related to damage in the form of microcracks. It is fundamental that the law governing the evolution of damage be related to the mechanical energy input to the ice.

If mechanical energy is input to a small volume of ice, it can result in the following effects:

(i) There can be an increase in the elastic strain energy (basically an increase in internal energy).

(ii) The work can be dissipated as heat during creep processes. These do not usually result per se in substantial changes to the structure of the material, although grain boundary sliding leads to stress concentrations and consequent crack initiation.

The zones near a crack tip (Figure 5.4) are zones of high shear stress with associated high rates of creep.

(iii) There can be frictional dissipation across crack faces (Figure 5.4).

(iv) The work can be used in processes resulting in damage to the material. We will be concerned primarily with the creation of new surfaces by cracking.

The damage processes in item (iii) represent a distinct case: the work is largely dissipated in the region of intense high stresses near the crack tip as the crack advances. Not all is dissipated, however. Some energy is conserved as surface energy but this is a small percentage (about 10%) of the energy dissipated and cannot readily be regained. For practical purposes, the energy in damaging the material can be treated as being dissipated but to refer to the energy as being entirely dissipated is not correct.

Consider the stress-strain relation illustrated in Figure 5.10. Given an initial stress, s, and shear modulus, G, an increment of strain, de, is applied to a volume of ice. This increment is applied rapidly such that the ice responds elastically and damages but does not creep. The damage results in a decrease of the modulus by an amount, dG, and does not leave any residual strains. The initial elastic strain energy was

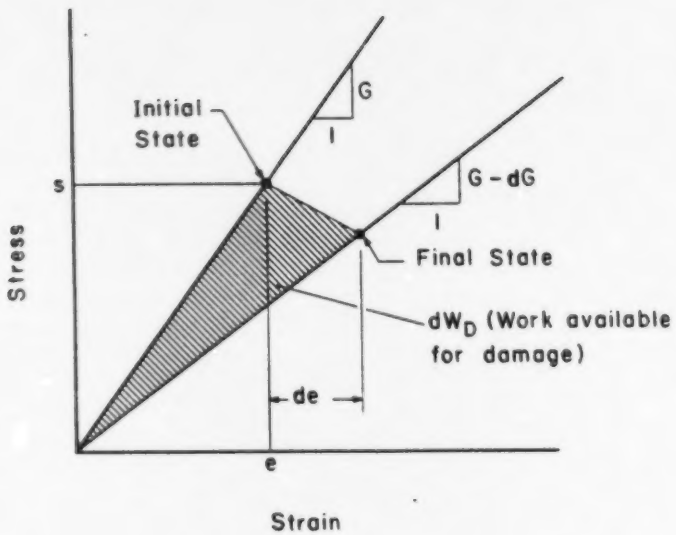

Figure 5.10. Uniaxial stress-strain representation for a purely elastic damaging material.

$$E = \frac{1}{2}\,\frac{s^2}{G}\,, \tag{5.8}$$

obtained by integrating the stress-strain curve, and the mechanical energy added was

$$\frac{1}{2}[s+(G-dG)(\frac{s}{G}+de)]de. \tag{5.9}$$

By summing (5.8) and (5.9) and subtracting the remaining elastic energy, based on G-dG, the amount of energy that is available for damage is

$$dW_D = \frac{1}{2} \frac{s^2}{G} \frac{dG}{G} , \tag{5.10}$$

ignoring products of the small strain increment, de, and the resulting small change in elastic modulus, dG. Recalling equation (5.7), the rate of damage can be simply expressed for the uniaxial situation as

$$\dot{\lambda} = \dot{\lambda}(W_D, E). \tag{5.11}$$

Future experimental work should focus on damage evolution as a function of the rate of energy input to ice samples under combined states of stress. This will aid in the parameterisation of the damage evolution law (equation (5.7) or (5.11)).

6. FLOW OF CRUSHED MATERIAL

6.1 Evidence of Pulverised Ice

There is considerable evidence of the presence of a pulverised layer of ice adjacent to the indenter face when ice is subject to brittle failure in compression. This thin layer of crushed ice particles has been found in many impact tests (e.g. Kheisin and Cherepanov, 1970; Comfort and Menon, 1981; Kawakami et al. 1983; Garcia et al. 1985). It tends to be pasty at temperatures close to freezing and dry at lower temperatures. In continuous indentation, pulverised ice is extruded from the face of the indenter as long as brittle compressive failure is a dominant mechanism (e.g. Michel and Blanchet, 1983; Sodhi and Morris, 1986; Timco, 1986). The same mechanism has been observed in recent tests with spherical indenters and also against Gulf's Molikpaq structure in the Beaufort Sea (e.g. Jefferies and Wright, 1987).

The thickness of the pulverised layer varies from only a few millimeters in laboratory tests (e.g. Timco, 1986) to more than an order of magnitude greater against the Molikpaq. Many laboratory and field tests show that the layer is distinct from the neighbouring microfissured ice. For continuous indentation, the pulverised particles are squeezed out at the points of lowest confining pressure. When the speed of the indenter is constant, the force against the

indenter varies rapidly. This observation is universal for fast indentation tests. Timco and Jordaan (1987) found an approximate relation between the particle distribution and the spectral density of the time varying force. This may appear obvious, but it is an important guide in the development of a conceptual model.

Another feature of the force-time variation is the shape of the oscillation. While the rising and falling portions may sometimes consume the same time, a long oscillatory rise is frequently followed by a sudden drop. This is illustrated in Figure 5.2. The sudden decrease in force is associated with the release of elastic strain energy stored in the ice, forming a dense array of microcracks. The slower rising force is the result of the failure and subsequent flow of the densely fractured ice. Since the pressure is greatest immediately adjacent to the indenter, this is where the ejection occurs.

Very little has been written on the flow of crushed ice. Only Kurdyumov and Kheisin (1976), Kheisin et al. (1975), Cormeau et al. (1986), Jordaan and Timco (1987), Tunik, (1984, 1987) and Nevel (1986) have begun to address this problem. There exist no published experimental results on the flow of pulverised ice under the confining pressures present during crushing. Further insight must therefore be drawn from the behaviour of broken ice in shear box tests and from the flow of brash ice. Fortunately, many other granular materials have also been studied extensively.

The following sections address the geotechnical and flow properties of ice and other granular materials. In the last section, current theories on the flow of pulverised ice are outlined.

6.2 Mohr-Coulomb Properties of Crushed Ice

Since crushed ice has very little cohesion, its geotechnical characteristics can be well described by its shear behaviour. The results of "shear box" tests are summarized in Table 6.1. The relation between shear and normal stresses is given by the friction angle, ϕ. as shown in the typical graph from Hellman (1984) given in Figure 6.1.

Table 6.1 Summary of shear box tests on broken ice particles

Authors	Ice type	Particle Size (m)	Velocity (ms^{-1})	Normal Shear σ (kPa)	Friction Angle ϕ (degrees)
Gale et al. (1985)	dry -1°C	.003	$.5x10^{-5}$ $.2x10^{-5}$	50-150	45
Hellman (1984)	mush fresh	.02-.04	.001-.1	4	40-60
Fransson and Sandkvist (1985)	brash	.10-.15	.01	15	14-34
Prodanovic (1979)	saline rubble	.02-.04	.0001-.01	<3	50
Keinonen and Nyman (1978)	model	.02-.04	-	<2	47

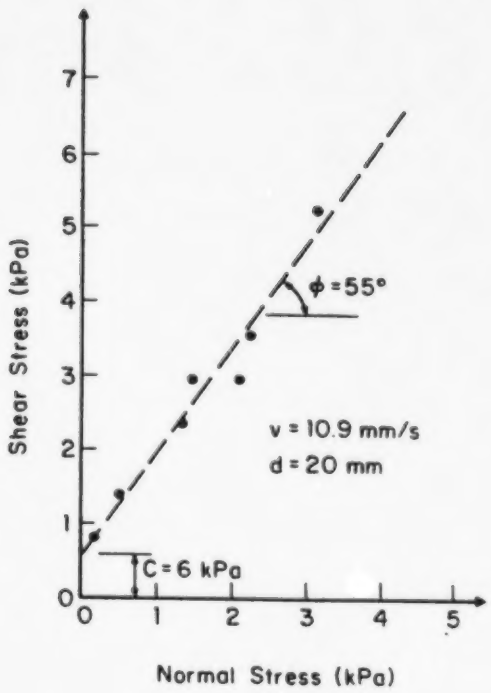

Figure 6.1. Typical results from shear box tests. The dots represent experimental data, and the friction angle, ϕ, and cohesion, C, are the best-fit Mohr-Coulomb parameters.

There was a significant variation in the particle size between the tests; this is particularly important in the Fransson and Sandkvist (1985) case since the overall dimensions of the shear box were only 0.5 m square. Water comprising one fifth of the volume was also present in this test, thereby increasing pore pressure and causing the decrease in the friction angles. Cohesion was not a significant factor in any of the tests. In spite of the discrepancy in the shear velocity between

Gale et al. (1985) and Hellman (1984), the friction angles were consistently in the 40 to 50 degree range. This range is the same as that obtained by Prodanovic (1979) for ice rubble and in the summary given by Mellor (1980).

In a biaxial apparatus under plane strain conditions, Sayed (1987) has analysed the compressive failure of a broken ice mass. Although the goal of this study was related to ice pileup and ridging, the results summarised in Table 6.2 are nevertheless of interest here. The friction angles are in line with the shear box results of Gale et al. (1985), Hellman (1984) and the rubble tests of Prodanovic (1979).

It would be speculative to translate the results found here to the behaviour of pulverised ice. First of all, the pressures involved in the geotechnical tests are one to three orders of magnitude less than the crushing pressures found by Timco (1986) and Bohon and Weingarten (1985). The velocities involved are similarly smaller than those that would produce brittle failure in continuous indentation.

The concept of treating the failure of crushed ice as a Mohr-Coulomb material has some merit. This approach can be used to predict the initiation of flow of the crushed particles; it does not however account for the frictional dissipation once flow occurs. This important consideration is addressed in Sections 6.3 and 6.4. For the static case, a friction angle of 45 degrees is suggested, but this in

no way obviates the need to conduct further tests on small particles at the velocities and confining pressures present during impact and continuous indentation.

Table 6.2 Summary of confined rubble compression tests by Sayed (1987). Particle size varied from .03 m to .07 m.

Temperature ^{o}C	Strain Rate (s^{-1})	Confining Pressure σ (kPa)	Cohesion C (kPa)	Friction Angle ϕ (Degrees)
-10	6.7×10^{-4}	10-50	10-20	50
	1.7×10^{-3}	10-80	10-20	40
-22	3.3×10^{-4}	10-70	20	40
	1.7×10^{-3}	10-70	10-20	30

6.3 Theory of the Flow of Granular Materials

Pulverised ice has many attributes that make it similar to other granular materials. The particles are distinct and size distributions can be measured. Collisions between particles exhibit elastic properties and the contact geometries result in frictional resistance. In many cases, it can be considered as a "dry" material and therefore no interparticle fluid needs to be considered.

Pulverised ice is also unique. Ice is brittle and the particles

will continue to damage even under the hydrostatic condition of flow. As the melting point of ice is approached, the particles are lubricated by a water film. This difference was observed by Kheisin and Cherepanov (1970) from the texture of the damaged ice subsequent to impact.

A comprehensive review on the flow of granular materials is given by Savage (1983). From the analysis of many granular materials, the viscosity of the interparticle fluid is not relevant as long as the particle density is sufficient. This is always the case for pulverised ice in crushing. Crushed ice can therefore be considered as a "dry" material. For slow flow, Savage (1983) categorises dry granular materials as quasi-static and recommends the use of a Mohr-Coulomb analogy which is frequently used for soil behaviour. The Mohr-Coulomb theory defines a failure state from the difference between the maximum and minimum principal stresses that is independent of hydrostatic pressure.

Extensive experiments on the shear flow of dry granular materials were made by Savage and Sayed (1984) using an annular shear cell. The particles were approximately 1 mm in diameter with static friction angles, ϕ, of 23^{o} to 35^{o}. The tests yielded relations between shear rate, shear stress and normal stress at maximum stresses of about 1 kPa, for constant values of void ratio. The dynamic equivalent to the friction angle, the ratio of shear to normal pressures, was up to 50

percent greater than in the static case.

Another summary of the mechanics of granular materials for flow in hoppers and bins is given by Brown and Richards (1970). For these materials, the static Mohr-Coulomb theory is found adequate and the concept of a critical void ratio to produce flow is advanced. Slip surfaces were found to be distinct, indicating the preference of granular materials to flow as a plug, with sharp discontinuities at the boundaries. The initiation of flow was found to be dependent on the geometry of the particle packing; the flow itself was not well described.

Similar flow regimes are found in snow avalanches. The models proposed for snow (e.g. Eglit, 1983; Lang et al., 1984) are typically Bingham flow, with shear stress,

$$\tau = \tau_o + \mu(\frac{dv}{dy})^n, \tag{6.1}$$

where τ_o is the static shear stress, v is the avalanche velocity, y is the snow thickness coordinate, n is a constant and μ is a nonlinear viscosity of the form

$$\mu = \mu_o(1+c\rho^{-\beta v}), \tag{6.2}$$

where μ_o, c and β are constants. The linear Bingham fluid (i.e. n=1,

c=0) is illustrated in Figure 6.2, contrasting it with Newtonian and non-Newtonian flow. Note that, for n=0, a velocity independent plastic flow is modelled by (6.1).

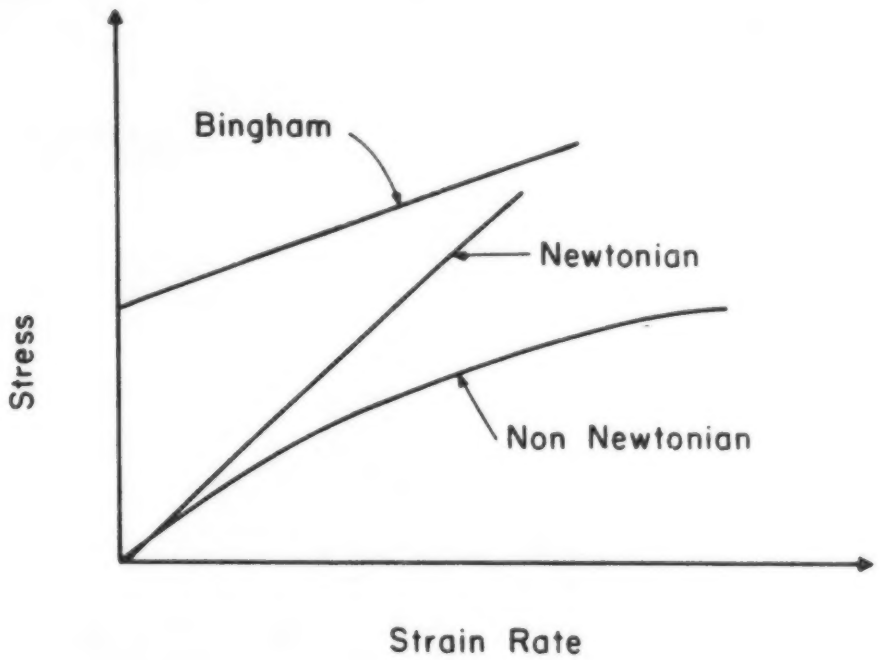

Figure 6.2. Schematic showing the behaviour of Bingham "locking", Newtonian and non-Newtonian fluids.

The above reviews also address the question of boundary conditions for granular materials. The thickness of the bounder layer in a granular material is a function of the particle size and the roughness of the adjacent material, in addition to the frictional characteristics

of the particles. The literature on granular materials therefore offers some good ideas for the analysis of crushed ice. It does not, however, consider stresses in the same order of magnitude that are present during the extrusion of pulverised ice particles during impact and indentation.

6.4 The State of the Art: Flow of Crushed Ice

No concensus has been reached on the best way to model the flow of the pulverised layer during extrusion. This is primarily due to lack of research effort. What is evident is that this layer is thin relative to the width of the indenter (e.g. Sodhi and Morris, 1986; Timco and Jordaan, 1987; Kheisin and Cherepanov, 1970). This has prompted the use of a flow analogy with appropriate simplifications from lubrication theory because of the small layer thickness (Kheisin et al., 1975; Kurdyumov and Kheisin, 1976; Jordaan et al., 1987; Jordaan and Timco, 1987).

The problem of a rectangular indenter has been considered by Jordaan and Timco (1987). The problem is illustrated in Figure 6.3, in which an ice sheet of thickness, h, is continuously indented at a velocity, v_o, by an indenter of width, d. The coordinate axis, y, is normal to the face of the indenter and the axis, x, is tangential, oriented vertically, with the origin at mid-width and mid-thickness of the ice. The equations for Newtonian viscous flow in the two

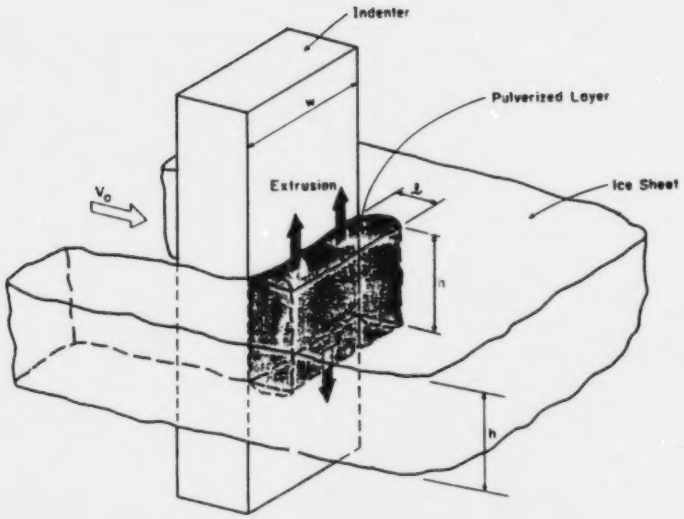

(a)

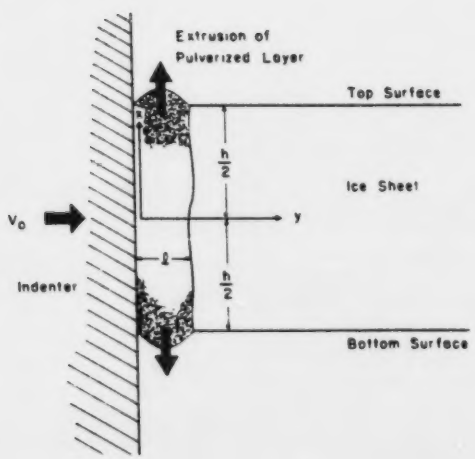

(b)

Figure 6.3. (a) Continuous indentation experiment,
(b) Cross-section perpendicular to the face of the indenter.

coordinate directions, simplified using the thin layer approximation, reduce to

$$\frac{\partial p}{\partial x} = \mu \frac{\partial^2 u}{\partial y^2} \tag{6.3}$$

and

$$\frac{\partial p}{\partial y} = 0, \tag{6.4}$$

where p is pressure, μ is the effective viscosity of the crushed ice and u(x,y) is the flow velocity tangential to the indenter face. It was assumed that the pressure only varied significantly in the vertical (x direction, see Figure 6.3) direction and $\partial^2 y/\partial v^2$ was much larger than $\partial^2 u/\partial x^2$. Continuity of flow was established by

$$\frac{\partial u}{\partial x} = \frac{-\partial v}{\partial y}, \tag{6.5}$$

where v is the velocity normal to the face of the indenter. It was assumed that variation of v normal to the indenter exceeded that tangential to it, i.e. v=v(y). The boundary conditions used by Jordaan and Timco (1987) for the solution of (6.5) are $u(x,0) = u(x,\ell) = 0$, i.e. no-slip conditions at both boundaries; $v(0)=v_o$ and $v(\ell)=0$. By virtue of symmetry about the mid-depth of the ice sheet, u(0,y)=0 was

specified. The resulting solutions were

$$u(x,y) = 6v_o(\frac{y}{\ell^2})(1 - \frac{y}{\ell})x \tag{6.6}$$

in the vertical, tangential to the face of the indenter, and

$$v(y) = v_o(1 - 3\frac{y^2}{\ell^2} + 2\frac{y^3}{\ell^3})x \tag{6.7}$$

in the horizontal, normal to the indenter face. Assuming that the pressure at the top and bottom surfaces of the ice was negligible, i.e. $p(h/2)=0$, the pressure on the face of the indenter as a function of x was calculated from (6.3) as

$$p(x) = \frac{\mu v_o}{\ell}(\frac{h}{\ell})^2 (\frac{1}{4} - \frac{x}{h})^2 \quad . \tag{6.8}$$

At this point, the layer thickness can vary as a function of x in (6.3). If, however, a constant layer thickness is assumed, then the net force on the indenter can be obtained by the suitable integration of (6.8) over the face of the indenter and is given by

$$F = \mu v_o(\frac{h}{\ell})^3. \tag{6.9}$$

Note the inverse third power relation between the force and the layer thickness. Jordaan et al. (1987) have also calculated the same solution in the case of a spherical indenter.

Jordaan and Timco (1987) and Jordaan et al. (1987) look at the problem of continuous indentation. The pressure is calculated from the equations of flow as a result of the extrusion of crushed ice. In contrast, Kurdyumov and Kheisin (1976) and Kheisin et al. (1975) look at a static case and consider only the maximum pressure under a dropped spherical weight. They assume that the peak pressure is proportional to the layer thickness, ℓ. Note the fundamental difference between this assumption and the result (6.8) from Jordaan and Timco (1987) (and a similar one for a spherical indenter in Jordaan et al. (1987)) in which the pressure is proportional to $1/\ell^3$.

Tunik (1984, 1987) has applied the results of Kurdyumov and Kheisin (1976) to look at ice impact pressures for different geometries of ships and structures. Maximum pressures exerted by icebergs and multiyear ice against vertical structures were calculated to be approximately 20 MPa.

Nevel (1986) used the example of a dropped steel ball to compare the viscous approach (Kurdyumov and Kheisin, 1976) to a simpler constant strength theory. In the latter approach, the initial momentum of the ball is assumed to be resisted by a constant crushing pressure

during the penetration. Only small differences in maximum forces and pressures were noted for the two theories.

The pressure applied to the crushed layer is also a function of the stiffness of the damaged ice behind it. The pressures exerted on the structure or the indenter are therefore the result of the interaction between the extruding ice and the damaging ice behind it; neither one is alone responsible. Since the speed at which the elastic stress is propagated in the damaging ice far exceeds that in the extruding ice, the damaging ice would be primarily responsible for the peak indentation pressures. The discontinuous nature of the pressure that is transmitted is not surprising when each of the interacting processes has a minimum pressure required to initiate it. The damage process has a limiting energy as outlined in Chapter 5. The flow of crushed ice, although modelled as a continuous fluid process in this section (e.g. Jordaan and Timco, 1987) also may show the discontinuous locking behaviour outlined in section 6.3.

6.5 Suggested Procedures for Impact Testing

At this time, there is still speculation on the theory of flow for crushed ice. Some suggestions are therefore made here to guide data collection during indentation and impact testing. These supplement the comments relating to impact in section 4.2.

(i) It is important to look at the variation of the crushed layer thickness as indentation proceeds. An increase in pressure will speed the extrusion of crushed material and decrease the thickness of the layer. At the same time, the pressure increase will create more crushed ice through the damage mechanism. It is this balance that produces the time series variation in indentation pressure.

(ii) It is not sufficient to consider only the total specific energy during impact testing; this is not a unique index but depends on the degree of confinement of the sample. The measurement of the crushed layer thickness variation over time during impact, coupled with the measurement of contact pressures, will allow the energy dissipation during extrusion to be calculated. This is essential for apportioning the specific energy to damage in crushing and to clearing of the pulverised material. A particle size distribution is also important for relating crushing energy and crack density.

(iii) Understanding the flow of crushed ice is important because it is a major energy sink in the crushing process. The assumption of Newtonian flow for the extruding material is unsubstantiated experimentally; it has been selected because of its simplicity. The measurement of the flow properties of pulverised ice is therefore recommended.

(iv) The literature on the static properties crushed ice and other granular materials at low confining pressures indicates a Mohr-Coulomb behaviour. It is worth investigating the possibility of this type of mechanism at higher confining pressures; it may be important in the initiation of the flow.

(v) A further aid to understand the flow properties of crushed ice is to mark the ice during impact testing to get a better idea of the velocity profile in the crushed layer.

7. CONCLUDING REMARKS

7.1 Conclusions

Research on the engineering behaviour of ice, particularly with respect to brittle failure, is still in its infancy. Yet crushing is a significant factor in ice impact with ships, floating structures and fixed structures. A sign that research is catching up with the problem is when predictions can be made with some accuracy; ice, however, still holds many surprises.

Because of its brittleness, rate and temperature characteristics, ice is a material with few close relatives. At low strain rates, it is a complex viscoelastic material; it does not obey conventional plastic failure laws. For strain rates exceeding $10^{-3}s^{-1}$, it exhibits brittle, damaging characteristics. Again, it does not display plastic attributes and therefore cannot be characterised using conventional engineering analysis techniques. Fortunately, the damaging behaviour of other materials such as rocks, concrete and ceramics has been studied and provides some useful insights.

Brittle compressive failure of the ice is a significant mechanism during impact and indentation under moderate confining pressures. This can occur for icebreakers in breaking or ramming situations, and for iceberg and pack ice impacts with structures. In controlled experiments and recorded incidents of impact and continuous

indentation, two basic characteristics of the ice behaviour emerge. These are:

(i) Damage: elastic stress builds up in the intact ice and, at a certain threshold, microcracks form at a rate governed by the localized flux of mechanical energy. It is believed that most of the damage is due to shear, while tensile cracks propagate when possible away from the damaged area. The latter cracks may result in spalling when local confining pressures are low. The shear damage is characterised by a dense array of microcracks, substantially degrading the elastic properties of the ice. This is the cause of sudden drops in the applied pressure under continuous indentation.

(ii) Ejection of pulverised ice: once damage of the ice is complete due to coalescence of the microcracks, the particles are displaced against the impact or indenter surface. When a sufficient layer of pulverised ice has built up, it begins to flow and is ejected adjacent to the surface.

The interaction of the processes described in (i) and (ii) is the key to the calculation of pressures in brittle compressive failure. The peak pressure is governed by the damage mechanism in the ice mass, but the time varying pressure is due to the interaction of the damage and ejection processes.

7.2 Recommendations

Both experimental and theoretical aspects of brittle ice response were considered in this review. Based on the above understanding of the damage and pulverised ice ejection processes, the following recommendations are made to guide future analysis and testing efforts.

With regard to the theory, the primary goal is to predict ice pressures during impact and indentation. This requires, not only a fundamental understanding of the mechanics of ice crushing, but also a well founded approach for implementing these ideas in design formats. The proposed approach is the following:

(i) Ice load model: a practical method is required for establishing design guidelines. From anticipated ice properties and impact conditions, a physically or empirically based model is required to predict ice pressures on specified ship or structure geometries. The approaches used by Riska and Frederking (1987) and Daley (1987) are examples of this kind of model for use with ship hull geometries; they should therefore be assessed with regard to the theory described in points (ii), (iii) and (iv) that follow.

(ii) Continuum damage: it is impossible to deal explicitly with all the microcracks formed during brittle compressive failure. A continuum damage model is therefore suggested to evaluate

stresses in progressively damaging ice.

(iii) Crack mechanisms: to guide the development of the damage model in (ii), a more fundamental understanding of crack properties is required. This involves the prediction of crack lengths and densities, and an analysis of the dissipational properties that influence the coalescence of cracks.

(iv) Flow of crushed ice: this problem involves the establishment of conditions under which flow is initiated and an analysis of the ejection of the pulverised material. A more fundamental understanding of the properties of the flow is required. Appropriate boundary conditions and a relation between the layer thickness and the applied pressure also need to be investigated.

Since the scope of the review was primarily related to impact and indentation tests, some suggestions are made here to guide current and future experimental work. No specific test program is recommended; rather, guidelines are outlined so that the key elements of the mechanisms involved in ice crushing can be isolated.

(i) Ice condition: a detailed observation of the progression of failure processes in the ice during the test and the subsequent state of the ice are recommended; this is an important guide for the development of conceptual and theoretical models.

(ii) Degree of damage: both the progression during testing and final state of the crack density, patterns, length and void space should be measured. Without this information, the development of a physically based damage model is impossible.

(iii) Ice confinement: The multiaxial stress state of the ice should be investigated; it is the key for controlling the spread of damage and therefore obtaining peak pressures. In impact tests, this might involve the measurement of reaction forces, stress and strain in various parts of the ice sample. For continuous indentation, the stress and strain states in the ice sheet or bulk sample and the stiffness of the indenter should be measured. Triaxial tests at high strain rates ($>10^{-2}s^{-1}$) under moderate confinement would be useful.

(iv) Energy control: the control of mechanical energy to an ice sample is a key ingredient in apportioning energy to damage and the flow of crushed ice. This can be accomplished in a closed loop triaxial setup and by the measurement of energy sinks during impact and indentation.

(v) Flow of crushed ice: the layer thickness and motion of the crushed ice should be measured as impact and indentation tests progress and related to the pressures on the impact or indenter face. In an independent series of experiments, the viscosity and flow properties of pulverised ice should be evaluated.

Finally, it should be re-emphasised that experiments be designed not only to measure ice pressures, but also to isolate the fundamental mechanisms that are associated with them.

8. REFERENCES

8.1 Textbooks on Impact and Damage

Billington, E.W. and Tate, A. (1981). "The Physics of Deformation and Flow". McGraw Hill.

Bridgman, P.W. (1941). "The Nature of Thermodynamics". Harvard.

Brown, R.L. and Richards, J.C. (1970). "Principles of Powder Mechanics". Pergammon Press, 221p.

Cottrell, A.H. (1964). "The Mechanical Properties of Matter". Wiley.

Cottrell, A. (1975). "An Introduction to Metallurgy". Edward Arnold.

Goldsmith, W. (1960). "Impact". Edward Arnold, London.

Hill, R. (1950). "The Mathematical Theory of Plasticity". Oxford.

Lemaitre, J., and Chaboche, J.L. (1985). "Mécanique des Matériaux Solides". First Edition, Dunod.

Love, A.E.H. (1927). "A Treatise on the Mathematical Theory of Elasticity". Cambridge University Press.

Johnson, W. (1972). "Impact Strength of Materials". Edward Arnold, London.

Michel, B. (1978). "Ice Mechanics". Les Presses de l'Universite Laval, Quebec.

Pounder, E.R. (1965). "The Physics of Ice", Pergammon Press.

Timoshenko, S.P., and Goodier, J.N. (1970). "Theory of Elasticity". Third Edition, McGraw Hill.

8.2 References Cited in the Report

Ackley, S.F. (1973). "Microhardness Testing on Single Ice Crystals". In Physics and Chemistry of Ice, (eds. E. Whalley, S.J. Jones and L.W. Gold), Royal Society of Canada, Ottawa.

Ashby, M.F. and Hallam, S.D. (1986). "The Failure of Brittle Solids Containing Small Cracks Under Compressive Stress States". Acta Metallurgica, Vol. 34, No. 3, pp.497-510.

Ashby, M.F. and Duval, P. (1985). "The Creep of Polycrystalline Ice". Cold Regions Science and Technology, Vol. 11, pp.285-300.

Barbee, T.W. Jr., Seaman, L., Crewdson, R. and Curran, D. (1972). "Dynamic Fracture Criteria for Ductile and Brittle Metals". Journal of Materials, JMLSA, Vol. 7, No. 3, pp.393-401.

Bohon, W.M. (1984). "Forces Exerted by Ice Failing in Crushing". Proc. 3rd. OMAE Symp., New Orleans, Vol. 3, pp.187-195.

Bohon, W.M. and Weingarten, J.S. (1985). "The Calculation of Ice Forces on Arctic Structures". Proc. Conference Arctic '85, Civil Engineering in the Arctic Offshore, San Francisco, pp.456-464.

Boklen, R. (1973). "A Simple Method for Obtaining the Ductility from a 100°-Cone Impression", In Science of Hardness Testing (ed. J.H. Westbrook and H. Conrad), American Society for Metals, 109-116.

Brooks, P.N. (1975). "The Influence of Static Mechanical Properties on the Resistance of Fresh-Water Ice to Ballistic Penetration, Report 4032/75, Defence Research Establishment, Valcartier, Quebec, 29p.

Butkovitch, T. (1954). "Microhardness of Single Ice Crystals". USA SIPRE Research Report 9.

Comfort, G. and Menon, B. (1981). "Laboratory Investigation of Ice Impact Pressure". Arctec Canada Ltd., report submitted to Ship Safety Branch, Canadian Coast Guard.

Cook, R.F., Lawn, B.R. (1984). "Controlled Indentation Flaws for Construction of Toughness and Fatigue Master Maps". Methods for Assessing the Structural Reliability of Brittle Materials, ASTM STP 844, S.W. Freiman and C.M. Hudson, Eds., American Society for Testing and Materials, Philadelphia, 1984, pp.22-42.

Cormeau, A., Jordaan, I.J. and Maes, M. (1986). "Development of a Model for Progressive Damage in Ice". Report submitted to the Department of Public Works, Ottawa.

Croasdale, K.R., Morgenstern, N.R. and Nuttal, J.B. (1977).

"Indentation Tests to Investigate Ice Pressures on Vertical Piers". J. Glaciology, Vol. 19, No. 81, pp.301-312.

Croft, S., Kieffer, S. and Ahrens, T. (1979) "Low Velocity Impact Craters in Ice and Ice-Saturated Sand with Implications for Martian Crater Count Ages". J. Geophys. Res., Vol. 84(B14), 8023-8032.

Daley, C. (1987) "Analysis of Ice Penetration Data in Support of Parametric Physical Modelling". Arctec Canada Ltd. report for Canadian Coast Guard, Vol. 1, 146p., Vol. 2, 87p.

Dougill, J.W. (1983). "Path Dependence and a General Theory for the Progressively Fracturing Solid". Proc. R. Soc. Lond., A390, 341-351, Great Britain.

Dougill, J.W. (1983). "Constitutive Relations for Concrete and Rock. Applications and Extensions of Elasticity and Plasticity Theory". William Prager Symposium on Mechanics of Geomaterials, Rocks, Concretes, Soils, September 11-15.

Dougill, J.W., Lau, J.C., and Burt, N.J. (1976). "Towards a Theoretical Model for Progressive Failure and Softening in Rock, Concrete and Similar Materials". To be presented at the American Society of Civil Engineering Mechanics Division Specialty Conference of Mechanics in Engineering University of Waterloo, Ontario, May 26-28.

Dougill, J.W. (1975). "Some Remarks on Path Independence in the Small in Plasticity". Quarterly of Applied Mathematics, October.

Dougill, J.W. (1976). "On Stable Progressively Fracturing Solids". Reprint from Journal of Applied Mathematics and Physics, Vol. 27, Fasc. 4, ZAMP, pp. 423-437.

Dougill, J.W., and Rida, M.A.M. (1980). "Further Consideration of Progressively Fracturing Solids". The Journal of Engineering Mechanics Division, October.

Eglit, E.M. (1983). "Some Mathematical Models of Snow Avalanches", in Advances in the Mechanics and Flow of Granular Materials, (ed. M. Shahinpoor), 577-588.

El-Tahan, H., Swamidas, A.S.J., Arockiasamy, M. and Reddy, D.V. (1984). "Strength of Iceberg and Artificial Snow Ice Under High Strain Rates and Impact Loads". Proc. of OMAE '84, pp.158-165.

Evans, A.G., Palmer, A.C., Goodman, D.J., Ashby, M.F., Hutchison, J.W., Ponter, A.R.S. and Williams, G.J. (1984). "Indentation Spalling of Edge-Loaded Ice Sheets". IAHR Ice Symposium, Hamburg. pp.113-121.

Fonseka, G.U. and Krajanovic, D. (1981). "The Continuous Damage Theory of Brittle Materials", Part 2: Uniaxial and Plane Response Modes, Journal of Applied Mechanics, Vol. 48, pp.816-824.

Forrestal, M.J. and Longcope, D.B. (1982). "Closed Form Solutions for Forces on Conical-Nosed Penetrators into Geological Targets with Constant Shear Strength", Mechanics of Materials I, pp.185-295.

Forrestal, M.J., Longcope, D.B. and Norwood, F.R. (1981). Journal of Applied Mechanics, Vol. 48, pp.25-29.

Fransson, L. and Sandkvist, J. (1985). "Brash Ice Shear Properties-Laboratory Tests". Proc. Symposium on Port and Ocean Engineering under Arctic Conditions, Narssarssuaq, Greenland, pp.75-87.

Gale, A.D., Sego, D.C. and Morgenstern, N.R. (1985). "Geotechnical Properties of Ice Rubble, Report 1". Report for the Natural Sciences and Engineering Research Council of Canada.

García, N.B., Farrell, D. and Mellor, M. (1985). "Ice Penetration Tests". Cold Regions Research and Engineering Technology, 11, pp.223-235.

Gerard, R. (1976). "A Simplified Measure of Ice Strength". Third International Symposium on Ice Problems, IAHR, Hanover, NH, U.S.A.

Glen, I.F. and Comfort, G. (1983). "Ice Impact Pressure and Load Investigation by Laboratory Experiment and Ship Trials", Proc. of POAC '83, Helsinki, pp.516-533.

Gold, L.W. (1972): "The Failure Process in Columnar-Grained Ice". NRCC Paper No. 369.

Goodman, D.J. (1980). "Critical Stress Intensity Factor (K_{IC}) Measurements of High Loading Rates for Polycrystalline Ice". In. P. Tryde (Ed.), Physics and Mechanics of Ice, IUTAM Symp., pp. 129-146.

Hamza, H. and Muggeridge, D.B. (1979). "Plane Strain Fracture Toughness (K_{IC}) of Fresh Water Ice". Proc. POAC '79, Norwegian Inst. of Tech., Trondheim.

Hellman, J.H. (1984). "Basic Investigations on Mush Ice". Proc, IAHR Symposium on Ice Problems, Hamburg, West Germany, pp.37-55.

Hightower, M.M., Norwood, F.R. and Young, C.W. (1982) "Development of an Ice Penetrometer Model", Report SAND82-0599, Sandia National Laboratories, Albaquerque, New Mexico, 47p.

Hirayama, K., Schwarz, J. and Wu, H. (1974). "An Investigation of Ice Forces on Vertical Structures", Iowa Inst. of Hydraulic Research Report No. 158, The Univ. of Iowa, Iowa City, Iowa.

Holsapple, K.A. and Schmidt, R.M. (1982). "On the Scaling of Crater Dimensions, 2. Impact Processes", Journal of Geophysical Research, Vol. 87, No. B3, pp.1849-1870.

Itagaki, K. and Sabourin, R.L. (1980). "Fracture Behaviour of Ice in Charpy Impact Testing". CRREL Report 80-13, 13p.

Jefferies, M.G. and Wright, W.H. (1987) . "Dynamic Response of Molikpak to Ice-Structure Interaction", Proc. OMAE '88, Houston, Vol. IV, pp.201-220.

Johnson, R.C. and Benoit, J.R. (1987) "Iceberg Impact Strength". Proc. of 19th Offshore Technology Conference, Houston, 417-423.

Jones, S.J. (1982). "The Confined Compressive Strength of Polycrystalline Ice". Journal of Glaciology, Vol. 28, No. 98, pp.171-177.

Jordaan, I.J. (1986). "Numerical and Finite Element Techniques in Calculation of Ice-Structure Interaction". 8th. IAHR Symposium on Ice, Iowa City, August.

Jordaan, I.J. (1986a) "Fracture Mechanics and Damage Theory as a Basis for Calculation of Ice-Structure Loads", NRC Workshop on Extreme Ice Features, Banff, Alberta, Proceedings, 1987.

Jordaan, I.J. (1987). Reply to Discussion, Proceedings IAHR (Iowa City), Vol. III (in press).

Jordaan, I.J. and McKenna, R.F. (1988). "Constitutive Relations for Creep of Ice", in preparation.

Jordaan, I.J. and Timco, G.W. (1987). "Dynamics of the Ice Crushing Process". Draft Manuscript.

Jordaan, I.J., Maes, M.A. and Nadreau, J.-P. (1988). "The Crushing and Clearinf of Ice in Fast Spherical Indentation Tests", Proc. OMAE '88, Houston, Vol. IV, pp.111-116.

Kawakami, S., Mizutami, H., Tagaki, Y., Kato, M. and Kamazawa, M. (1983) "Impact Experiments on Ice". J. Geophys. Res., Vol. 88(B7), 5906-5814.

Keinonen, A. and Nyman, T. (1978). "An Experimental Model-Scale Study on the Compressible, Frictional and Cohesive Behaviour of Broken Ice Mass". Proc. IAHR Symposium on Ice Problems, Lulea, Sweden.

Kheisin, D.E. and Cherepanov, N.V. (1970). "Change of Ice Structure in the Zone of Impact of a Solid Body Against the Ice Cover Surface", in Problemy Arktiki i Antarktiki, 34.

Kheisin, D.E. and Likhomanov, V.A. (1973). "An Experimental Determination of the Specific Energy of Mechanical Crushing of Ice by Impact". Problemy Arktiki i Antarktiki, Vol. 41, pp.69-77.

Kheisin, D.E., Likhomanov, V.A. and Kurdyumov, V.A. (1975). "Determination of Specific Breakup Energy and Contact Pressures Produced by the Impact of a Solid against Ice". U.S. Army Cold Regions Research and Engineering Laboratory. TL539. English Translation.

Korzhavin, K.N. (1962). "Action of Ice on Engineering Structures". Publishing House of Siberian Branch of USSR Academy of Sciences (English translation, CRREL, 1971).

Krajcinovic, D., and Fonseka, G.U. (1981). "The Continuing Damage Theory of Brittle Materials". Journal of Applied Mechanics, December, Vol. 48.

Krajcinovic, D. (1984). "Continuum Damage Mechanics". Applied 4 Mechanics Reviews, Vol. 37, No. 1, pp.1-6.

Kry, P.R. (1979a). "High Aspect Ratio Crushing Tests". APOA Report 093-01.

Kry, P.R. (1979b). "Stress Distributions During Crushing of Ice". APOA Report 148-01.

Kry, P.R. (1978). "A Statistical Prediction of the Effective Ice Crushing Stresses on Wide Structures", IAHR Symposium on Ice Problems, Lulea, Sweden, Vol. 1, pp.33-47.

Kry, P.R., Lucente, R.F., Hedley, R.E. (1978). "Continuous Crushing of Ice". APOA Report 106-01.

Kurdyumov, V.A. and Kheisin, D.E. (1976). "Hydrodynamic Model of the Impact of a Solid on Ice". Prikladnaya Mekhanika, Vol. 12, No. 10, pp.103-109.

Lang, T.E., Nakurama, T., Dent, J.D. and Martinelli, M. Jr. (1985). "Avalanche Flow Dynamics with Material Locking", Annals of Glaciology, pp.5-8.

Lawn, B.R., Evans, A.G. and Marshall, D.B. (1980). "Elastic Plastic Indentation Damage in Ceramics. The Median/Radial Crack System". Journal of the American Ceramic Society, Vol. 63, No. 9-10.

Lawn, B. and Wilshaw, R. (1975). "Review - Indentation Fracture. Principles and Applications". Journal of Materials Science 10, pp.1049-1081.

Leckie, F.A. (1978). "The Constitutive Equations of Continuum Creep Damage Mechanics". Philosophical Transactions of the Royal

Society, London, Series A, 288, 27-47.

Leckie, F.A. and Hayhurst, D.R. (1974). "Creep Rupture of Structures". Proceedings of the Royal Society, London, Series A., Vol. 340, 1974, pp.323-347.

Lemaitre, J., and Chaboche, J.L. (1978). "Aspect Phénomenologique de la Rupture par Endommagement". Journal de Mécanique Appliquée, Vol. 2, pp.317-365.

Liaw, B.M., Kobayashi, A.S. and Emery, A.F. (1984). "Theoretical Model of Impact Damage in Structural Ceramics". Journal of the American Ceramic Society, Vol. 67, No. 8, pp.544-548.

Likhomanov, V.A. and Kheisin, D.E. (1971). "Experimental Investigation of Solid Body Impact on Ice". Problemy Arktiki i Antarktiki, Vol. 38, pp.128-136.

Liu, H.W. and Miller, K.J. (1979). "Fracture Toughness of Fresh-Water Ice", Journal of Glaciology, Vol. 22 (86), pp.135-143.

Määttänen, M. (1983) "Dynamic Ice-Structure Interaction during Continuous Crushing". CRREL Report 83-5, 53p.

Marshall, D.B. and Lawn, B.R. (1980). "Flaw Characteristics in Dynamic Fatigue - The Influence of Residual Contact Stresses", Journal of the American Ceramic Society, Vol. 63, No. 9-10.

McIntosh, J.A., Young, C.W. and Walsh, J.P. (1973) "Development of a Sea-Ice Penetrometer". Journal of Petroleum Technology, Vol. 25, 249-256.

Mellor, M. (1980) "Ship Resistance in Thick Brash Ice". Cold Regions Science and Technology, Vol. 3, 305-321.

Michel, B. and Blanchet, D. (1983). "Indentation of an S2 Floating Ice Sheet in the Brittle Range". Annals of Glaciology 4, pp.180-187.

Michel, B. and Toussaint, N. (1977). "Mechanisms and Theory of Indentation of Ice Plates". J. of Glaciology, Vol. 19, No. 81, pp.285-300.

Neill, C.R. (1976). "Dynamic Ice Forces on Piers and Piles. An Assessment of Design Guidelines in the Light of Recent Research". Can. J. Civ. Eng., Vol. 3, pp.305-341.

Nevel, D.E. (1986). "Iceberg Impact Forces". Proc. IAHR Symposium, Iowa City, Iowa.

Parsons, B.L. and Snellen, J.B. (1985). "Fracture Toughness of Fresh Water Prototype Ice and Carbamide Model Ice", Proc. POAC '85,

Narssarssuaq, Greenland, pp.128-137.

Ponter, A.R.S. et al. (1983). "The Force Exerted by a Moving Ice Sheet on an Offshore Structure, Part 1 - The Creep Mode". Cold Regions Sci. Tech., 8, pp.109-118.

Prodanovic, A. (1979). "Model Tests of Ice Rubble Strength". Proc. Symposium on Port and Ocean Engineering under Arctic Conditions, Trondheim, Norway, pp.89-105.

Ralston, T.D. (1978). "An Analysis of Ice Sheet Indentation". Proc. IAHR Symposium on Ice Problems, Part 1, Lulea, Sweden, pp.13-31.

Ralston, T.D. (1979). "Sea Ice Loads", in Technical Seminars on Alaskan Beaufort Sea Gravel Island Design, Exxon Production Research Company.

Resende, L., and Martin, J.B. (1983a). "A Progressive Damage Continuum Model for Granular Materials". Computer Methods in Applied Mechanics and Engineering 42 (1984) 1-18 North Holland.

Resende, L., and Martin, J.B. (1983b). "Damage Constitutive Model for Geotechnical Applications". University of Cape Town, Rondebosch, Cape Town, South Africa, Nonlinear Structural Mechanics Research Unit, Technical Report No. 44.

Resende, L. and Martin, J.B. (1984). "A Progressive Damage 'Continuum' Model for Granular Materials". Computer Methods in Applied Mechanics and Engineering, Vol. 42, pp.1-18.

Riska, K. and Frederking, R. (1987) "Ice Load Penetration Modelling". Proceedings POAC 87, Fairbanks, Alaska.

Ross, B. (1967). "Penetration and Fracture of Sea due to Impact Loading", in Physics of Snow and Ice, (ed. H. Oura), Proc. of Intl. Conf. on Low Temperature Science, Hokkaido University, Sapporo.

Ross, B. (1969). "Perforation of the Arctic Sea-Ice Cover by Projectile Impact". Journal of Hydronautics, Vol. 3, No. 3, July.

Rychnovsky, R. (1987). "Deep Ice Penetrator". Proc. 9th. Int. Conf. on Port and Ocean Engineering under Arctic Conditions, Fairbanks, Alaska.

Savage, S.B. (1983). "The Mechanics of Rapid Granular Flows". In Advances in Applied Mechanics, Vol. 24, pp.289-366.

Savage, S.B. and Sayed, M. (1984). "Stresses Developed by Dry Cohesionless Granular Materials Sheared in An Annular Shear Cell". J. Fluid Mech., Vol. 142, pp.391-430.

Sayed, M. (1987). "Mechanical Properties of Model Ice Rubble". Sixth Annual Structures Congress, ASCE.

Schapery, R.A. (1964). "Application of Thermodynamics to Thermomechanical, Fracture, and Birefringent Phenomena in Viscoelastic Media". J. of Applied Physics, Vol. 35, No. 5.

Shockey, D.A., Curran, D.R., Seaman, L., Rosenberg, J.T. and Petersen, C.F. (1974). "Fragmentation of Rock Under Dynamic Loads", Int. Journal Rock Mechanics Science and Geomechanics, Vol. 11, pp.303.

Sinha, N.K. (1978). "Short-Term Rheology of Polycrystalline Ice". J. of Glaciology, Vol. 21, No. 85, pp.457-473.

Sjolind, S.-G. (1987). "A Constitutive Model for Ice as a Damaging Visco-Elastic Material", Cold Regions Science and Technology, No. 41, pp.247-262.

Sodhi, D.S. and Morris, C.E. (1984) "Ice Forces on Rigid, Vertical, Cylindrical Structures". CRREL Report 84-33, 47p.

Sodhi, D.S. and Morris, C.E. (1986) "Characteristic Frequency of Force Variations in Continuous Crushing of Sheet Ice against Rigid Cylindrical Structures". Cold Regions Science and Technology, Vol. 12, 1-12.

Spooner, D.C., and Dougill, J.W. (1975). "A Quantitative Assessment of Damage Sustained in Concrete During Compressive Loading". Reprinted from Magazine of Concrete Research, Vol. 27, No. 92, September, pp.151-160.

Taylor, G.I. (1946). "Testing of Materials at High Rates of Loading". Journal Inst. Civil Engineers (London), Vol. 26, pp.486-519.

Tillett, J.P.A. (1955). "Fracture of Glass by Spherical Indenters", Proc. Phys. Soc. LXIX, I-B, pp.47-54.

Timco, G.W. and Frederking, R.M.W. (1986). "Flexural Strength and Fracture Toughness of Sea Ice". Cold Regions Sci. and Technol., 8.35-41.

Timco, G.W. (1986). "Indentation and Penetration in Freshwater Ice". Proceedings of 5th. Symposium on Offshore Mech. and Arctic Eng., OMAE, Japan, April 13-17, pp.444-452.

Timco, G.W. (1987). "Ice/Structure Interaction Tests with Ice Containing Flaws", Journal of Glaciology, Vol. 33, No. 114, pp.186-194.

Timco, G.W. and Jordaan, I.J. (1987). "Time Series Variations in Ice Crushing". Proc. 9th. Intl. Conference on Port and Ocean Under Arctic Conditions, Fairbanks, Alaska.

Timco, G.W. and Martin, R.A. (1979). "Impact Strength Tests on Ottawa River Ice", National Research Council Canada, Division of Mechanical Engineering Report LTR-LT-97, 20p.

Tomin, M.J., Cormeau, A., Jordaan, I.J., (1985). "Development of Analytical Models Related to Experimental Work on Ice Structure Interaction". Report by Det norske Veritas to Department of Public Works, Government of Canada.

Tomin, M., Cormeau, A. and Jordaan, I.J. (1986). "Experimental and Theoretical Study of Ice-Structure Interaction", Veritas Rep. No. 1985-CGY-036.

Tsuchiya, M., Kanie, S., Ikejiri, K., Yoshida, A. and Saeki, H. (1985) "An Experimental Study on Ice-Structure Interaction". Proc. 17th Offshore Technology Conference, Houston, 321-327.

Tunik, A.L. (1984). "Dynamic Ice Loads on a Ship", IAHR Ice Symposium, Hamburg, pp.297-313.

Tunik, A.L. (1987). "Impact Ice Loads on Offshore Structures", Proceedings of POAC '87, Fairbanks, Alaska.

Urabe, N., Iwasaki, T. and Yoshitake, A. (1980). "Fracture Toughness of Sea Ice". Cold Regions Sci. and Tech., 3, pp.29-37.

Varsta, P. (1983). "On the Mechanics of Ice Load on Ships in Level Ice in the Baltic Sea". Technical Research Centre of Finland, Publication 11, Espoo, 91pp.

Wang, Y.S. and Poplin, J.R. (1981). "Large Scale Ice Strength Tests, 1980". Exxon P.R.C. 23PR81.

Yen, Y-C, et al. (1970). "Impact of Spheres on Ice". Proc. A.S.C.E., Eng. Mech. Division, Vol. 36, No. EM5, October.

Young, C.W. (1974). "Penetration of Sea Ice by Air-Dropped Projectiles", Proc. IEEE Conf. on Eng. in the Ocean Environment, Halifax, N.S., Vol. 1, 89-95.

Zabilansky, L.J., Nevel, D.E. and Haynes, F.D. (1975). "Ice Forces on Model Structures", Canadian Journal of Civil Engineering, Vol. 2, pp.400-417.

8.3 Other References on Impact and Damage of Solids

Bazant, Z.P., and Gambarova, P.G. (1984). "Crack Shear in Concrete Crack Band Microplane Model", Journal of Structural Engineering, Vol. 110, No.9, pp.2015-2035.

Bazant, Z.P. (1977). "Endochronic and Classical Theories of Plasticity in Finite Element Analysis". International Conference on Finite Elements in Nonlinear Solid and Structural Mechanics, Geilo, Norway, Aug. 29-Sept. 1, Vol. 1.

Bazant, Z.P. (1976). "Instability, Ductility, and Size Effect in Strain-Softening Concrete". Journal of the Engineering Mechanics Division, April.

Bazant, Z.P., and Bhat, P.D. (1976). "Endochronic Theory of Inelasticity and Failure of Concrete". Journal of the Engineering Division, August.

Bazant, Z.P., and Krizek, R.J. (1975). "Endochronic Constitutive Law for Inelastic Shear and Densification of Sand". Proceedings of the Fifth Canadian Congress of Applied Mechanics, Fredericton, New Brunswick.

Burt, N.J., and Dougill, J.W. (1977). "Progressive Failure in a Mode Heterogeneous Medium". Journal of the Engineering Mechanics Division, June.

Carpinteri, A., and Sih, G.C. (1983). "Damage Accumulation and Crack Growth in Bilinear Materials with Softening. Application of Strain Energy Density Theory". Lehigh University, Institute of Fracture and Solid Mechanics, Report No. IFSM-83-115.

Chaboche, J.L. (1979). "The Continuous Damage Mechanics. A Tool to Describe Phenomena Before Crack Initiation". 2nd. Int. Seminar on Incl. Analysis and Life Prediction in High Temp. Env., pp.C9-C14.

Chen, E.P., Kipp, M.E., and Grady, D.E. (1984). "A Strain-Rate Sensitive Rock Fragmentation Model", in Mechanics of Oil Shale, edited by K.P. Chong and J.W. Smith, Applied Science Ltd.

Croasdale, K.R. (1980). "Ice Forces on Fixed, Rigid Structures". Part II in the Working Group on Ice Forces on Structures, A State-of-the-Art Report, Edited by T. Carstens, CRREL Special Rep. 80-26.

Davison, L., and Stevens, A.I. (1973). "Thermomechanical Constitution of Spalling Elastic Bodies". Journal of Applied Physics, Vol. 44, pp. 667-674.

Dienes, J.K. "Fracture, Failure, and Fragmentation". Theoretical

Division, Group T-3, Los Alamos National Laboratory, Los Alamos, New Mexico.

Hamza, H. (1986). "Application of Fracture Mechanics Techniques to Ice-structure Interaction Problems". IAHR Symposium, Iowa City, Vol. 1, pp.329-347.

Hayhurst, D.R., Dimmer, P.R., and Chernuka, M.W. (1975). "Estimates of the Creep Rupture Lifetime of Structures Using the Finite-Element Method". Journal of Mechanics and Physics of Solids, Vol. 23, pp.335-355.

Hirayama, K. (1974). "An Investigation of Ice Forces on Vertical Structures", Ph.D. Thesis, Department of Mechanics and Hydraulics, University of Iowa, 153p.

Horii, H., and Nemat-Nasser, S. (1982). "Overall Moduli of Solids with Microcracks. Load Induced Anisotropy". J. Mech. Phys. Solids, Vol. 31, pp.155-171.

Kachanov, L.M. (1958). "Time to Failure Under Creep Conditions". Isz. AN SSR OTN, No. 8.

Karr, D.G. (1985). "Constitutive Equations for Ice as a Damaging Material". Proc. Civil Eng. in the Arctic Offshore, ASCE, San Francisco, March 25-57.

Lange, M. and Ahrens, T. (1982) "Impact Cratering in Ice and Ice-Silicate Targets. an Experimental Assessment (abstract)". Lunar and Planetary Science, XIII, 417-418.

Mellor, M. (1983). "Mechanical Behaviour of Sea Ice". CRREL Rep. 83-1.

Morris, C.E. and Sodhi, D.S. (1984). "Crushing Ice Forces on Cylindrical Structures", IAHR Ice Symposium, Hamburg.

Nemat-Nasser, S., and Horii, H. (1984). "Micro-Mechanics of Fracture and Failure of Geo-Materials in Compression". Advances in Fracture Research, Proceedings of the 6th International Conference on Fracture (ICF6), New Delhi, India, Dec. 4-10.

Nemat-Nasser, S., and Horii, H. (1984). "Rock Failure in Compression". Int. J. Engrg. Sci., Vol. 22, No. 8-10, pp.9499-1011.

Nemat-Nasser, S., and Horii, H. (1982). "Growth of Microcracks in Rocks, and Load-Induced Anisotropy". Symposium on Fracture Mechanics Approach to Hydraulic Fracturing and Geothermal Energy, Sendai, Japan, November 8.

Palmer, A.C. et al. (1983). "Fracture and its Role in Determining Ice

Forces on Offshore Structures". Annals of Glaciology, pp.216-221.

Riska, K. and Daley, C. (1986) "Physical Modelling of Ship/Ice Interaction, Report 1 for Transport Canada and Ministry of Trade and Industry of Finland, 54p.

Sanderson, T.J.O. (1984). "Theoretical and Measured Ice Forces on Wide Structures". Proceedings, IAHR Symposium, Hamburg, Vol. IV, pp.151-207.

Sih, G.C. (1973). "A Special Theory of Crack Propagation in Mechanics of Fracture, Methods of Analysis and Solution of Crack Problems". Ed. G.C. Sih, Noordhoff.

Sinha, N.K. (1984). "Intercrystalline Cracking, Grain-Boundary Sliding, and Delayed Elasticity at High Temperatures". Journal of Materials Science, Vol. 19, pp.359-376.

Stankowski, T., and Gerstle, K.H. (1983). "Simple Formulation of Concrete Behaviour Under Load Histories". Paper submitted for Publication in Jnl. A.C.I., September.

Vakulenko, A.A. and Kachanov, M.L. (1971). "Continuum Theory of Cracked Media". Mekh Tverdogo Tela, Vol. 6, pp.159-166.

Willam, K.J., and Sture, S. (1985). "A Composite Fracture Model for Localized Failure in Cementitious Materials". Paper presented at second Symposium on the Interaction of Non-Nuclear Munitions with Structures, Panama City Beach, Florida, April.

Willam, K.J., Bicanic, N., and Sture, S. (1984). "Constitutive and Computational Aspects of Strain-Softening and Localization in Solids". Presented at A.S.M.E. - WAM'84 Symposium on Constitutive Equations: Micro, Macro and Computational Aspects", New Orleans, December 10-14.

Zhurkov, S.N., and Sanfirova, T.P. (1958). "The Relationship Between Strength and Creep in Metals and Alloys". Zhurnal Teoreticheskoi Fyziki, Vol. 28, No. 8.